Michael Lammer, BSc

# INVESTIGATIONS ON GENERATION OF ULTRA-PURE HYDROGEN BY THE STEAM-IRON PROCESS USING A TUBULAR REACTOR SYSTEM

**MASTERARBEIT**

zur Erlangung des akademischen Grades

Diplom-Ingenieur

Masterstudium Technische Chemie

eingereicht an der

**Technischen Universität Graz**

Betreuer

Assoc.Prof. Dipl.-Ing. Dr.techn. Viktor Hacker

Institut für Chemische Verfahrenstechnik und Umwelttechnik
der Technischen Universität Graz

Graz, Juli 2014

## EIDESSTATTLICHE ERKLÄRUNG

## *AFFIDAVIT*

Ich erkläre an Eides statt, dass ich die vorliegende Arbeit selbstständig verfasst, andere als die angegebenen Quellen/Hilfsmittel nicht benutzt, und die den benutzten Quellen wörtlich und inhaltlich entnommenen Stellen als solche kenntlich gemacht habe. Das in TUGRAZonline hochgeladene Textdokument ist mit der vorliegenden Masterarbeit identisch.

*I declare that I have authored this thesis independently, that I have not used other than the declared sources/resources, and that I have explicitly indicated all material which has been quoted either literally or by content from the sources used. The text document uploaded to TUGRAZonline is identical to the present master‘s thesis.*

Datum / Date

Unterschrift / Signature

# Acknowledgements

My thanks go to Prof. Viktor Hacker, who gave me the possibility to work in his workgroup and who always found time to discuss emerging situations. His guidance was always appreciated. I also want to thank Prof. Matthäus Siebenhofer in his function as head of the institute, as he supported the work under his auspices.

Many thanks also go to Stephan Nestl and Gernot Voitic. I always appreciated to discuss many of the interesting results of the experiments performed with them. Stephan Nestl in his function as supervisor has backed me in every aspect of my work.

Last but not least I would like to thank all my lab colleagues as well as Carmen Gehrer for their excellent support throughout the whole period of time working on my diploma thesis.

*Abstract*

Hydrogen is needed for a variety of technologies and applications, ranging from industrial chemical processes over food technologies to advanced mobility applications. The aim of this work was to investigate the steam-iron process for providing hydrogen gas of high purity. Through the experiments performed, the optimum operating conditions and the reactivity and stability of different contact mass compositions have been explored. By its double-step nature, the steam-iron process offers the possibility to use carbon monoxide, synthesis gas or contaminated hydrogen for the reduction of iron oxides in the contact mass. The excess gas can be easily captured. The following oxidation of iron with steam releases the pure hydrogen. Preliminary cycles to study the Fe-FeO-$Fe_3O_4$-$Fe_2O_3$ system are contained as well as the investigations of different contact mass compositions and the potential side reactions during reductions with synthesis gas. The experiments were performed at 600 to 750°C. To obtain information on the behaviour under increased pressure, oxidation experiments were performed at 8 to 10 bar. Generating hydrogen gas at high pressure offers the possibility of reducing costs by saving downstream compressors. Most of the redox cycles were performed with hydrogen as reductant and steam as oxidant. In the later experiments, also synthesis gas mixtures were used to reduce the contact mass. The developed measurement setup yielded hydrogen of high purity. The $H_2$ product flow contained less than 450 ppm of $CO_2$. No other impurities were detected in the flow.

*Zusammenfassung*

Wasserstoff wird für eine Vielzahl von Technologien und Anwendungen, angefangen von chemischen Industrieprozessen über Lebensmitteltechnologie bis hin zu fortschrittlichen Mobilitätsanwendungen, benötigt. Ziel dieser Arbeit waren Untersuchungen des Eisen-Dampf-Prozesses zur Bereitstellung von hochreinem Wasserstoff. Mittels der durchgeführten Experimente wurden einerseits die optimalen Betriebsbedingungen bestimmt und andererseits die Reaktivität und Stabilität verschiedener Kontaktmassezusammensetzungen erforscht. Der Eisen-Dampf-Prozess eröffnet dabei durch seinen zweistufigen Ablauf die Möglichkeit, zur Reduktion von Eisenoxiden in der Kontaktmasse Kohlenmonoxid oder Synthesegas bzw. verunreinigten Wasserstoff einzusetzen. Der Gasüberschuss kann einfach aufgefangen werden. Der folgende Teil des Zyklus, die Oxidation des Eisens mit Dampf, setzt den reinen Wasserstoff frei. Zyklen, um das System Fe-FeO-$Fe_3O_4$-$Fe_2O_3$ zu studieren werden ebenso behandelt wie die Untersuchung verschiedener Kontaktmassezusammensetzungen und die potentiellen Nebenreaktionen bei der Reduktion mit Synthesegas. Die Experimente wurden bei 600 bis 750°C durchgeführt. Oxidationsversuche bei Drücken von 8 bis 10 bar wurden durchgeführt, um das Verhalten bei höherem Druck zu erforschen. Das Bereitstellen von Wasserstoffgas bei hohen Drücken kann durch das Einsparen von nachgeschalteten Kompressoren potentiell Kosten senken. Die meisten Redox-Zyklen wurden mit Wasserstoff als Reduktionsmittel und Dampf als Oxidationsmittel ausgeführt. In den Experimenten wurden auch Synthesegasmischungen benutzt, um die Kontaktmasse zu reduzieren. Der entwickelte Messaufbau stellte Wasserstoff von hoher Reinheit bereit. Der $H_2$ Produktstrom enthielt weniger als 450 ppm $CO_2$. Keine anderen Verunreinigungen wurden im Gasstrom detektiert.

# Content

'Some piously record "In the beginning God", but I say "In the beginning hydrogen".'
– attributed to Harlow Shapley, Astronomer, 1885-1972

# 1 INTRODUCTION

## 1.1 Energy and $CO_2$

As conventional fuel demand is ever increasing [1], but resources are limited, alternative energy sources or energy vectors are developed. The increasing concentration of greenhouse gases in the atmosphere like $CO_2$ leads to additional challenges like global warming and climate change, which can be taken in account for flooding, drought and failure of crops. By burning hydrocarbons derived from decayed organisms, the amount of carbonaceous species in the atmosphere increases to a non-equilibrium proportion related to growth and decay of biomass. The resulting excess emission of $CO_2$ cannot be converted via photosynthesis and stays in the atmosphere. The so called “green energy” vectors aim for using only contemporary plant and animal products as energy sources. In this approach the $CO_2$ first is utilized in building up the organic matter, e.g. by photosynthesis, which is then converted to fuel and can again emit the $CO_2$.

Hydrogen as energy vector has high potential in shifting the $CO_2$ emission out of the urban centres as this fuel is low on emission, only water is generated by (electro-chemically) combusting $H_2$. Hydrogen can be produced outside of highly populated areas. Green hydrogen technologies can utilize renewable resources in order to generate hydrogen gas, which can then be converted into electric energy. Because of the demand for a sustainable energy system hydrogen technologies have recently offered a broad field of research in both chemical engineering [2] and bio technologies [3].

Fuel cell systems can convert the chemical energy contained in hydrogen gas into electric energy in a very efficient way [4]. Various types of fuel cells working under different conditions are subjects of research both for stationary, decentralized and for mobility applications. Systems operating at higher temperatures – high temperature fuel cells or solid oxide fuel cells – are generally more difficult in maintenance but also more resistant towards impurities in the fuel stream like CO and $CO_2$ than low temperature fuel cells. These cells – e.g. polymer electrolyte membrane FCs – are of high interest due to their relative simplicity of operation. For utilization of hydrogen in fuel cells, especially for low temperature FCs, a high purity of hydrogen is paramount [5]. Thus fuel processing and purification offer an extensive field of research.

## 1.2 Hydrogen Generation

The diatomic hydrogen molecule is the simplest molecule in the universe. Because of its reactivity and low density, the concentration of molecular hydrogen in the atmosphere of earth is insignificant. Though hydrogen containing species are abundant on our planet – liquid water, ice and vapour as well as hydrocarbon compounds and biological structures as carbohydrates, amino acids and fats – molecular hydrogen is not present [6].

Hydrogen is needed in industrial applications like petrochemical refining operations, metallurgical reduction processes and hydrating of fatty acids in food chemistry. Fischer-Tropsch synthesis as process for generating liquid hydrocarbons and ammonia synthesis via the Haber-Bosch process also rely heavily on technical produced hydrogen. For mobility and off-site energy storage and conversion, hydrogen storage coupled with fuel cell systems can improve atmospheric situations in urban areas, as the high emission industrial hydrogen production is located outside the city. Operating on bigger scale leads to higher efficiency, so converting hydrocarbons to hydrogen and then using the hydrogen in mobility applications improves the overall efficiency of traffic. There are also challenges occurring in hydrogen storage and transport due to gas diffusion through many materials and the necessity of maintaining very high pressure for reasonable energy density. Decentralized generation of $H_2$ presents an alternative. The implementation of the double-step steam-iron process offers an advantage due to hydrogen generation and an effective way of carbon capture and storage.

### 1.2.1 Generation from Water

**Electrolysis** of water makes use of electric energy to split it into molecular hydrogen and oxygen. The theoretically necessary potential is 1.229 V compared to the standard hydrogen electrode. Oxygen is generated at the anode (Equation 1) whereas hydrogen gas is generated at the cathode (Equation 2) of the electrolysis cell.

$$2\,H_2O \leftrightarrows O_2 + 4\,H^+ + 4\,e^- \quad (1)$$

$$4\,H^+ + 4\,e^- \leftrightarrows 2\,H_2 \quad (2)$$

The efficiency of water electrolysis is determined by the thermodynamic efficiency of the system as well as the efficiency of the respective electrolyser system. Efficiencies of 56 to 73 % are state of the art [7]. To achieve high conductivity necessary for electrolysis, inorganic salts like KOH are dissolved in the water. Due to the hydrogen over-potential, the potassium is not deposited at the negative electrode but molecular hydrogen is formed. Very high pressure of hydrogen can be reached by electrolysis. Depending on temperature and concentration up to 700 bar are reached, still operating at good conditions [8].

**Thermolysis** of water occurs only at very high temperatures well above 2000°C. Decomposition at this temperatures yields hydrogen which can be separated from steam and by-products like $H_2O_2$ by cooling and condensing these substances. The removal of oxygen from the product stream prevents the recombination of $H_2$ and $O_2$. Other gaseous components of the product gas stream can be removed by pressure-swing-adsorption.

$$H_2O \xrightarrow{\Delta T} H_2 + \frac{1}{2}O_2 \quad (3)$$

Although thermolysis of water is theoretically possible, it is not of significant importance for technical applications.

### 1.2.2 Generation from Hydrocarbons

The generation of hydrogen gas from hydrocarbons is mostly done by reforming operations. The most abundant catalytic species used in industrial application are nickel based compounds due to their high activities and low costs compared to noble metal catalysts [9].

In the field of hydrocarbon conversion, chemical looping processes [10, 11] can prevent the emission of carbonaceous products by use of an oxygen carrier. This carrier substance is permanently located in the reactor. In case of chemical looping combustion the oxygen chemically bound to the carrier is used up instead of an external oxygen source. To regenerate the fixed or fluidized bed, mostly a stream of air is used. This alternating oxidation and reduction of the oxygen carrier is characteristic for looping processes.

**Steam reforming** is a widely used method of producing hydrogen gas at temperatures of about 700 to 850°C by reaction of hydrocarbons, mainly methane, with steam (Equation 4). By use of a second reaction step even more hydrogen can be obtained, utilizing the water-gas-shift reaction (Equation 5). Nickel based catalysts allow this process to be performed at given temperatures. Research in this field focuses on the improvement of the catalytic system to achieve higher activity and economic benefits [12].

$$CH_4 + H_2O \leftrightarrows 3\,H_2 + CO \quad (4)$$

$$CO + H_2O \leftrightarrows H_2 + CO_2 \quad (5)$$

The endothermic reforming reaction is carried out at 850°C to yield hydrogen and carbon monoxide. Due to the exothermic character of the water gas shift reaction, lower temperatures are necessary. After cooling the product gas stream, the high temperature water gas shift reaction is performed. The low temperature water gas shift reactor is operated at even lower temperatures. This is a compromise between thermodynamic and kinetic influence which is used to achieve maximum conversion [13].

Steam reforming is currently one of the main sources for hydrogen but it suffers from several drawbacks. As fossil fuels might contain catalyst poisons like sulphur, eventually pretreatment is necessary if this is economically reasonable. Also energy input is quite high, as temperature has to be maintained at high levels during the operation.

As the reforming reaction (Equation 4) is endothermic and the shift reaction (Equation 5) is exothermic, different reactor systems are needed to prevent an overall limitation of the process. Galvita and Sundmacher [14] proposed a two-step process similar to chemical looping operations making use of platinum containing catalysts and separating the $H_2$ from the carbonaceous gas stream.

**Autothermal reforming** uses steam and oxygen to generate synthesis gas (Equation 6) of variable proportion of hydrogen to carbon monoxide. The term “autothermal” derives from the combination of an endothermic reforming and an exothermic partial oxidation. This partial oxidation of methane occurs at higher temperatures than steam reforming – at approximately 1000°C.

$$3\,CH_4 + H_2O + O_2 \leftrightarrows 7\,H_2 + 3\,CO \quad (6)$$

By implementing a water-gas-shift reactor, the carbon monoxide fraction can be reduced and more hydrogen can be obtained. Various different catalyst systems can be applied; the process is also applicable for reforming of other hydrocarbons and alcohols [9].

**Dry reforming** is a method similar to steam reforming. Instead of steam, carbon dioxide is used to oxidize the methane (Equation 7). An implemented water-gas-shift reactor increases the hydrogen output by partly converting the CO proportion to $CO_2$ (Equation 5). This is also possible in the way of a chemical looping dry reforming with a fixed bed of oxygen carrying contact mass [15]. This chemical looping dry reforming utilizes $CO_2$ for the reaction leaving CO as off gas, which is essentially not quite favourable. To drive the process mostly Ni-based catalysts are used. To prevent the formation of carbon deposits on the catalyst, the process must be designed in the adequate manner [16].

$$CH_4 + CO_2 \leftrightarrows 2\,H_2 + 2\,CO \quad (7)$$

In 2011 Oyama et al. [17] compared the dry reforming with steam reforming. At pressures higher than 5 atm, dry reforming will undergo the reverse water-gas shift reaction (Equation 8) due to higher reactivity of $H_2$ compared to $CH_4$. This leads to lower yields of hydrogen gas in the product stream and thus is not favourable.

$$H_2 + CO_2 \leftrightarrows CO + H_2O \quad (8)$$

**Steam reforming and purification with inorganic membranes** is a way to retrieve pure hydrogen from a hydrogen rich product stream [18]. The membrane consists of palladium based alloys or palladium, which is selectively permeable for hydrogen. By removing the hydrogen from the reaction site, according to Le Chatelier's principle conversion is enhanced.

From the scientific point of view this appears to be a good way of hydrogen purification, but there is a severe economic drawback – the price of palladium. In the last five years the price of palladium rose to about 800 $/oz t [19]. Utilizing metals of that price in widespread applications would surely lead to even higher prices sooner or later.

## 1.3 Generation from Hydrocarbons by Use of Iron and Iron Oxides

The steam-iron process purifies synthesis gas or uses other reductive gas mixtures for generating hydrogen of high purity. Originally following the so called Lane process and the consecutively developed Messerschmitt process at the dawn of the twentieth century the steam-iron process was used to generate hydrogen for airship filling in Europe where helium was scarce.

Nowadays it can yield ultra-pure hydrogen for fuel cell applications. Filling airships like the famous Hindenburg with hydrogen gas of moderate purity does not significantly affect the vehicle's performance as long as the hydrogen proportion is high enough to lift the airship off ground. Today hydrogen mobility and power storage and conversion programs purity is of much greater significance. Hydrogen oxidizing fuel cells such as PEM-FCs – proton exchange membrane fuel cells – need hydrogen free of contaminants. Even traces of carbon monoxide poison the platinum catalysts and therefore influence the lifetime of the cell.

Originally Howard Lane, a British engineer, developed a steam-iron reactor to produce hydrogen for aviation and industry [20]. These systems proved to be too complex. Lane plants could be operational for a few weeks during army manoeuvres, where a lot of soldiers could do the work but in industrial application the system was too expensive and difficult to operate. The German Anton Messerschmitt further changed the process to facilitate the operating procedure in a way of preventing premature sintering of the contact mass and thus enhancing the stability of the system and also optimized the heat distribution in the reactor [21].

Hydrogen was used for various processes and applications. In metallurgical and chemical processes it was used as general reducing agent. The newly invented Haber-Bosch process utilizes hydrogen for generating ammonia for agricultural fertilization and also military application for explosives. Militaries of the late 19$^{th}$ and early 20$^{th}$ century in Europe and also in the United States saw the sky as new field of operation and developed rigid airships and balloons to secure dominance in the air – mainly for reconnaissance and later during World War 1 also for bombing missions. For these aircraft helium and hydrogen were used as lifting gases. As political tensions grew in the first years of the 20$^{th}$ century, the later Central Powers were no longer able to rely on the helium resources of Russia, Africa and North America. For lifting the famous Zeppelins, hydrogen had to be employed. Due to huge developments in aviation technology and catastrophic setbacks like the crash of the Hindenburg in 1937, airships and balloons lost their importance in civilian traffic and military application. The airships where replaced by faster and more versatile fixed wing aircraft and generating huge amounts of hydrogen as lifting gas was no longer important.

But the need for hydrogen is not limited to agricultural and military development. Hydrogen is needed for metallurgical applications as a reductant and in food technologies for processing vegetable oils by hydrogenation. It is used as propellant for rockets and spacecraft and as energy storing medium for fuel cells and hydrogen combustion motors. Throughout the 20$^{th}$ century hydrogen was created by steam reforming, autothermal reforming or dry reforming. All of these methods produce a hydrogen-rich product gas stream – consecutive purification steps to remove carbon monoxide, carbon dioxide, nitrous oxides and hydrocarbon by-products are necessary for most applications. These cost intensive purification steps can be reduced by spatially separating the hydrogen production from the hydrocarbon oxidation.

The cyclic steam-iron process [22, 23] allows using renewable as well as fossil hydrocarbons as basis for generating and storing hydrogen. Due to its double-step nature, the product gas stream is not diluted with nitrogen. During the reduction step only steam and carbonaceous compounds leave the reactor, in the oxidation step hydrogen gas in steam is generated. Condensation of steam then separates the components and yields pure hydrogen. This kind of purification via two steps facilitates the possibility of carbon capture and storage.

Though the steam-iron process utilizes sponge iron as a contact mass as reactant for both reactions, they are performed discontinuously in two steps. Oxidation of the contact mass with steam releases hydrogen gas of high purity. As long as there are no contaminants deposited on the contact mass, only hydrogen gas and non-converted steam leave the reactor. Separating hydrogen from steam is performed by condensation. Reduction of the resulting oxides by a stream of reducing gases like synthesis gas or contaminated hydrogen again forms an oxidizeable contact mass. Supply of synthesis gas can be achieved by a methane reformer [24]. By operating in an alternating two-step mechanism the produced carbon dioxide, a product of the syngas oxidation, can be captured.

If the contact mass consists of highly oxidized iron such as hematite, the first reduction leads to magnetite (Equation 9), a species of lower oxidation state. Further reduction then gives wuestite (Equation 10) or metallic iron (Equation 11). Wuestite consecutively is also reduced to metallic iron (Equation 12). Reduction occurs also by use of carbon monoxide. The chemical reaction Equations are similar, as CO reacts in the same proportions as $H_2$ and forms carbon dioxide as product gas. Hematite can also be reduced to metallic iron by a stream of methane (Equation 13).

$$3\,Fe_2O_3 + H_2 \rightarrow 2\,Fe_3O_4 + H_2O \qquad \Delta H_{298} = \text{-17.0 kJ/mol} \qquad (9)$$

$$Fe_3O_4 + H_2 \rightarrow 3\,FeO + H_2O \qquad \Delta H_{298} = \text{+63.1 kJ/mol} \qquad (10)$$

$$Fe_3O_4 + 4\,H_2 \rightarrow 3\,Fe + 4\,H_2O \qquad \Delta H_{298} = \text{+153.7 kJ/mol} \qquad (11)$$

$$FeO + H_2 \rightarrow Fe + H_2O \qquad \Delta H_{298} = \text{+30.2 kJ/mol} \qquad (12)$$

$$Fe_2O_3 + CH_4 \rightarrow 2\,Fe + CO + 2\,H_2O \qquad \Delta H_{298} = \text{+302.9 kJ/mol} \qquad (13)$$

Oxidation of iron gives magnetite $Fe_3O_4$ (Equation 14) or wuestite FeO (Equation 15), which can be further oxidized to magnetite (Equation 16). As oxidation of the metallic contact mass occurs by steam, oxidation to hematite is thermodynamically hindered. The highest state of oxidations reachable in this setup is formal $Fe^{2.67+}$, magnetite $Fe_3O_4$.

$$3\,Fe + 4\,H_2O \rightarrow Fe_3O_4 + 4\,H_2 \qquad \Delta H_{298} = \text{-153.7 kJ/mol} \qquad (14)$$

$$Fe + H_2O \rightarrow FeO + H_2 \qquad \Delta H_{298} = \text{-30.2 kJ/mol} \qquad (15)$$

$$3\,FeO + H_2O \rightarrow Fe_3O_4 + H_2 \qquad \Delta H_{298} = \text{-63.1 kJ/mol} \qquad (16)$$

As the steam-iron-reactor is operated at temperatures of about 750°C thermal stability of the contact mass is paramount for the process. To achieve this goal, other metal oxides such as $Al_2O_3$ are added to the contact mass. In 1995 Popović et al. [25] investigated the formation of solid solutions of $Al_2O_3$ in $Fe_2O_3$. This additive can either be added to fine powders of iron oxide before forming contact mass pellets or precursor solutions like aluminium nitrate can be used to impregnate the highly porous sponge iron. Calcination of the contact mass then gives a powder with evenly distributed additive. This was done similar to the work of C.D. Bohn [26].

The stabilizing effect of added aluminium oxide was described by Topsøe et al. [27]. A formation of homogeneous particles consisting of iron oxide and aluminium oxide is achieved by the sample preparation and diffusion at high temperatures. During reduction of the contact mass, the iron oxide is reduced to metallic iron whereas the aluminium oxide is not reduced but forms inclusions of $FeO{\cdot}Al_2O_3$ insoluble in iron. These inclusions lead to material strain which in turn cracks the particles. Topsøe et al. proposed that these effects could prevent sintering of the contact mass.

The thermodynamic equilibrium of the respective reaction during an experiment is specified by the chemical species located closest to the reactor's exit. After the component with the highest oxidation state had been reduced to a lower state, another conversion is reached. This goes on until the whole contact mass is reduced to metal and no conversion of reductant takes place any more. The Baur-Glaessner chart [28] (Figure 1 – left) provides information on the various states of oxidation and the respective proportions of the gas mixtures $CO/CO_2$ and $H_2/H_2O$. High conversion of reductive gas indicates the reaction of highly oxidized species to lower oxidation states. Low conversion of reductant is thus related to reduction of species of low to even lower oxidation state. In Figure 1 – right, the conversion and volume flow of hydrogen uptake during a reduction experiment performed during this work is shown. An initial conversion of >95 % indicated the presence of hematite, the species of the highest oxidation state. Once all the hematite was converted, the magnetite phase's conversion was observable. The conversion rapidly decreased from about 60 % to 30 %. This is referred to the conversion of magnetite to wuestite. The molar amount of oxidic species increased during the previous reduction by the factor of 3, according to Equation 10. As three moles of FeO are formed from one mole of $Fe_3O_4$, the last reduction of wuestite to iron took about three times as long.

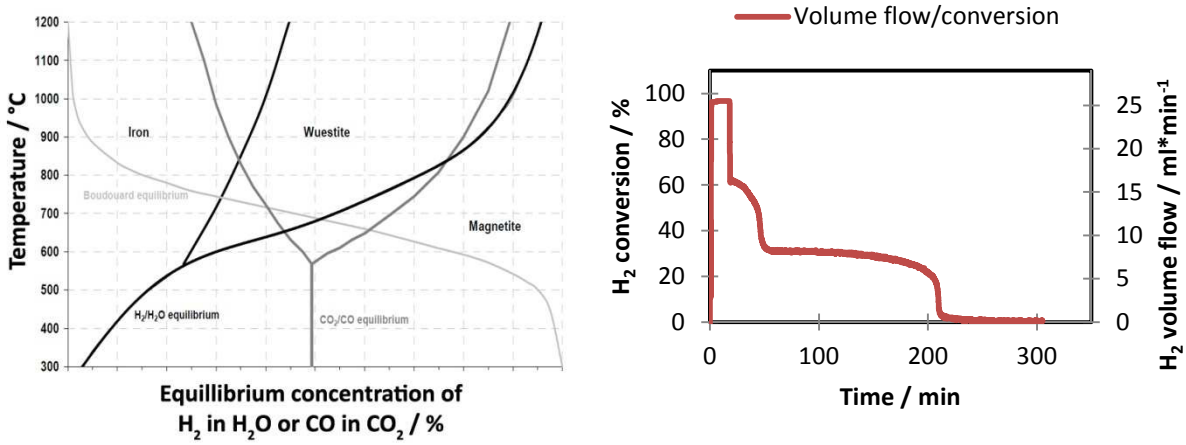


**Figure 1: Baur-Glaessner chart displaying equilibrium concentrations of reductive gases at various species as a function of temperature (left); reduction of $Fe_2O_3$ with 10 wt% of $Al_2O_3$ at 750°C with 25 ml/min of $H_2$.**

# 2 EXPERIMENTAL METHOD

## 2.1 Materials and Sample Preparation

The experiments were carried out with six types of contact masses, which were either self-prepared or made by Stephan Nestl and Gernot Voitic. The samples used are as follows:

- *Iron sponge*: porous iron powder by Alfa Aesar
- *Fe/$Al_2O_3$ 5%:* self-prepared from iron sponge, with 5 wt% of aluminium oxide
- *Fe/$Al_2O_3$ 10%:* self-prepared from iron sponge, with 10 wt% of aluminium oxide
- *Fe/$Al_2O_3$ 20%:* self-prepared from iron sponge, with 20 wt% of aluminium oxide
- V1kl1: Hematite $Fe_2O_3$
- *V7:* Hematite $Fe_2O_3$ with 10 wt% of aluminium oxide $Al_2O_3$
- *V2:* Hematite $Fe_2O_3$ with 10 wt% of aluminium oxide $Al_2O_3$

Different proportions of aluminium oxide were expected to alter behaviour during the redox cycles performed. The $Al_2O_3$ was expected to stabilize the contact mass and to prevent loss of reactivity due to the thermal and mechanical stress during the experiments [29].

The sponge iron based samples (*Fe/$Al_2O_3$ 5%, Fe/$Al_2O_3$ 10%, Fe/$Al_2O_3$ 20%)* were prepared by an impregnation method similar to the method described by C.D. Bohn [30]. Synthesis was done in a twin-neck flask with thermometer. A solution of aluminium nitrate nonahydrate of adequate concentration in deionised water was prepared in the flask; the sponge iron was then added. By heating to about 80°C the water was removed by slow evaporation. The dried raw product then was crushed in a mortar and heated to 350°C to decompose the nitrate and form the aluminium oxide. After approximately two hours the raw contact mass was transferred into a ceramic bowl and calcinated at 900°C to fully decompose any nitrate residues.

The contact masses V1kl1, V7 and V2 were mechanically mixed powders of $Fe_2O_3$ and $Al_2O_3$ pelletized with deionised water.

For use in a tubular reactor, the samples were again crushed and then sieved. Only the 90 to 125 µm fraction was chosen for the experiments. This ensured a continuous relation of particle diameter to reactor diameter throughout all performed experiments.

## 2.2 Reactor System and Analysis

All experiments were carried out in a tubular reactor with an automated test rig for catalytic activity tests (MICROACTIVITY-Reference by PID Eng&Tech, Spain), partly modified for the steam-iron-experiments. The test rig is divided in two main regions – the so-called "hot box" and the outer area (Figure 2).

**Figure 2: Interior of MICROACTIVITY-Reference – the hot box.**

### 2.2.1 Setup of the Test Rig

Within the hot box the main tubing and the reactor is located. This box is thermally insulated and during operation it was kept at 180°C for pre-heating the gases, allowing the supply of steam to the reactor without condensation in tubes and supporting the reactor heating. The reactor itself was heated by an electric resistance system and installed inside the hot box in e vertical position. A reactor bypass line was present in the system and could be switched by a six-port valve.

The rest of the experimental apparatus was considered the outer area. Gas supply from the compressed gas cylinders and the relevant mass flow controllers to dose the gas flows were situated outside the hot box. These mass flow controllers were operated either by an in-system touch screen or an operating software on a connected PC. This software could also be used to record the gas flows, the temperatures and other system parameters. Gases leaving the reactor and consecutively the hot box were led into the liquid-gas separator.

Gases were supplied via mass flow controllers (Bronkhorst high-tech, Netherlands) and mixed in the gas mixing station. This device connected the gas streams. The supplied gases were fed into a Hastelloy X tubular reactor (Parker Autoclave Engineers, USA) filled with contact mass (*Materials and Sample Preparation*) and powdered $SiO_2$ (Fluka Chemika, Quartz) as inert material. A check valve was installed inside the hot box downstream the mixing station to prevent steam being pressed out into the mixing chamber during oxidations at raised

pressure. Without the check valve steam would leave the hot box and condense in the mixing chamber – no pressure build-up would be possible.

The supply with steam was achieved by use of an HPLC pump (Gilson, France). This pump delivered the adequate volume flow of water into the test rig's evaporator. This device consisted of a helical steel tube in a capsule heated by an installed heating cartridge and controlled by a thermocouple type K wired into the test rig's control system. A check valve situated before the evaporator prevented gases leaving the system during the experiments in case of no steam generation. As the steam was generated at 200°C and fed into the tubing inside the hot box (180°C), even at higher pressure, evaporation would still be possible. This was essential for some of the oxidation experiments, as hydrogen production at raised pressure was investigated.

The excess flow of steam and the steam produced during the experiment were separated from the product gas flow in order not to damage the analysis system. The liquid-gas separator consisted of an electrically cooled tank. This was used to condense the steam at about 4 to 5°C and thus separate the water from the gases which were then analysed. By collecting the water and gradually releasing it, the system could operate in a continuous way.

The reactor was heated by an electric resistance furnace built into the test rig. Temperature was measured and controlled by type K thermocouples. To measure the reaction temperature, one thermocouple was inserted into the contact mass bed (Figure 3). In the hot box surrounding the reactor system and the piping, temperature was measured in the upper region; a second thermocouple was installed in close proximity to the auxiliary heating cord, which heated the tubing from evaporator to reactor inlet. At the evaporator itself the last thermocouple was installed.

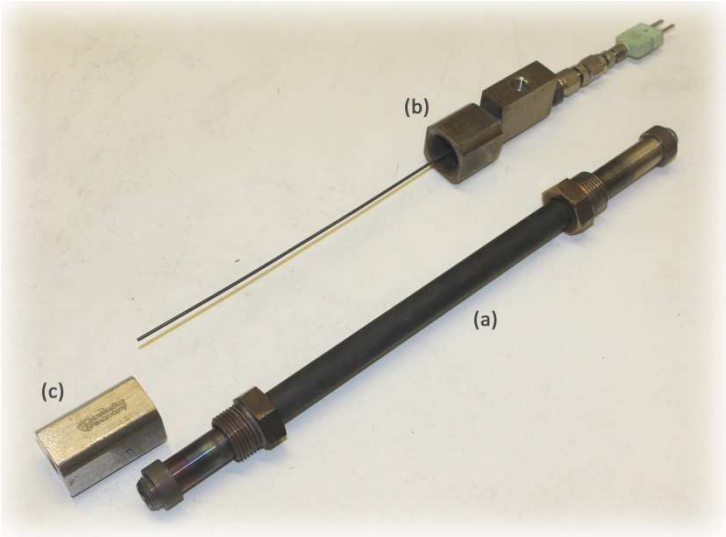


**Figure 3: Components of the reactor: (a) Main piece/reactor tube, (b) upper cap including thermocouple and connection to tubing, (c) lower cap including connection to tubing.**

For gas analysis three different systems were used. A thermal gas analyser, a micro gas chromatograph (Agilent, USA) and a mass flow controller (at first Vögtlin, Switzerland; then Bronkhorst high-tech, Netherlands) were implemented.

For experiments under increased pressure, pressure was built up by generation of hydrogen. The HPLC pump transported liquid water into the system, which then evaporated and increased the pressure. The reaction of steam to hydrogen had no significant influence on the pressure, as both components were gaseous. Non-converted steam is continuously condensed. Pressure does derive only from the product gas hydrogen as the contribution of steam is eliminated due to condensation. The pressure sensor was located before the reactor system; a needle valve at the gas exit of the test rig regulated the pressure inside the test rig. Alternatively pressure was built up by fully opening the needle valve and closing the following mass-flow controller. By these means the pressure build-up corresponded directly to the amount of generated hydrogen. By slowly opening the mass-flow controller during performing an oxidation reaction a constant flow could be achieved. This would only work with the MFC as analysis device, as it allows regulating the flow (Figure 4).

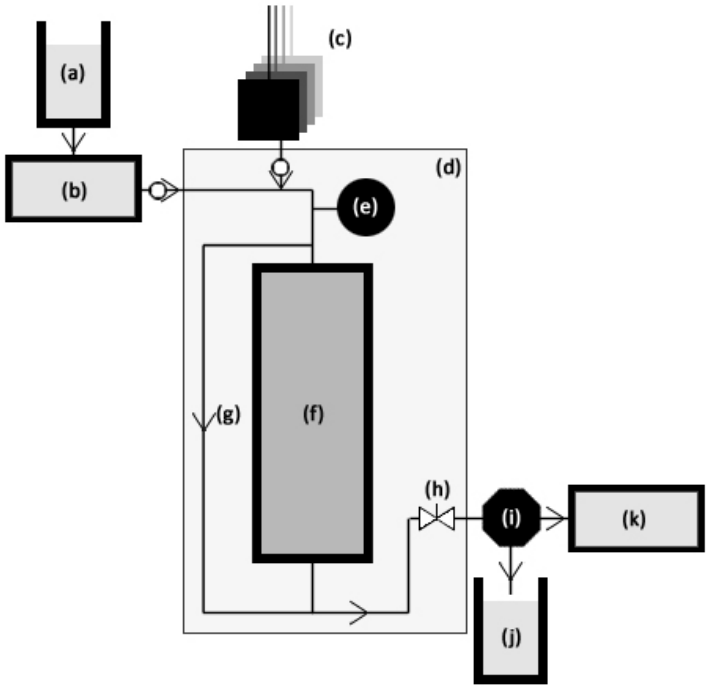


**Figure 4: Schematic view of MICROACTIVITY-Reference: (a) Water reservoir, (b) HPLC pump, (c) gas supply and mass flow controllers, (d) hot box, (e) pressure sensor, (f) reactor, (g) reactor bypass, (h) pressure regulating valve, (i) liquid-gas separator, (j) condensed water, (k) analysis system or MFC for pressure control.**

### 2.2.2 Preparation of the Reactor

The Hastelloy X tubular reactor (Parker Autoclave Engineers, USA) featured a sinter plate at half height, so contact mass and the inert material was filled in and removed from the top. This sinter plate was designed to hold the loading in place, as the reactor is installed in a vertical position. To prevent interaction of the contact mass with the sinter plate and mixing with the inert material, ceramic wool was used. Silicon dioxide (Fluka Chemika, Quartz) was used as inert material.

The first layer on the sinter plate was ceramic wool which acted as a spacer between the contact mass and the porous plate material. Onto that ceramic wool the contact mass bed was applied. The height of the reactive bed was determined by the powder density of the contact mass and chosen in a way to ensure the tip of the thermocouple was situated at the centre of that layer. Powder density was measured by weighing a certain volume (checked with a graduated cylinder) of contact mass. A second layer of ceramic wool held the contact mass bed in place and a silicon dioxide layer on top acted as a gas preheating zone. Distortion of this inert bed was prevented by another sheet of ceramic wool. A thermocouple for control of contact mass temperature was attached to the upper cap of the reactor and thus also was added from above. This thermocouple was fixed in length, so the contact mass bed had to be of the adequate height and also must not be tightly packed, as the thermocouple had to be pushed into the bed to allow measurement of the reaction temperature. As the contact mass bed was about 10 to 15 cm below the reactor's end, inserting the thermocouple was no trivial task, because of the possibility of not hitting the centre of the bed. This could lead to measurement errors related to the temperature (Figure 5), e.g. the reactor wall temperature. Also distortion of the fixed bed could occur by correcting the location of the thermocouple too often.

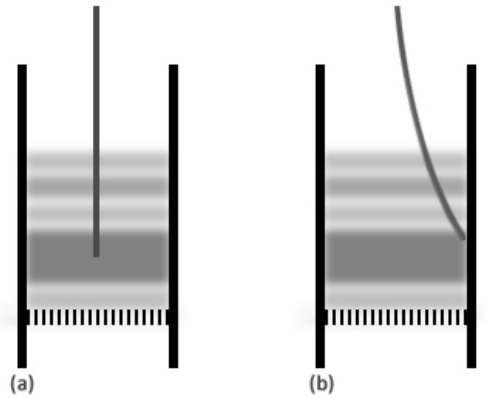


**Figure 5: (a) Thermocouple in the centre of the contact mass bed, (b) thermocouple bent to the side and touching the reactor wall.**

## 2.3 Test Procedure

An experimental series is defined as the sum of experiments performed with the same load of contact mass in the reactor. A series is subdivided into cycles, which themselves are subdivided into reduction and consecutively oxidation of the contact mass.

A series was started by loading the reactor with the contact mass in the way described in *Preparation of the Reactor*. The reactor was installed in the test rig and the thermocouple was connected to the control hardware. Possible leaks were identified by pressurizing the whole test rig up to 20 bar with nitrogen. A surfactant spray was used to find the locations of non-gastight connections. When the system was considered gastight, the hot box temperature was set to 180°C and the reactor to the relevant temperature described at the respective experiment's part. The evaporator's temperature was set to 200°C. The set temperatures allow the production of steam and the transport to the reactor without condensation.

Most cycles started with a reduction reaction performed. The outlet gas streams were detected and related to the inlet streams to calculate conversion rate and total gas amount.

The reactions' products also contained steam; the peltier cooled liquid-gas separator was used to condense the steam in order to protect the analysis system. Measurements in reactor bypass were performed to evaluate the base line for the experiment. The experiment was finished as soon as the volume flow of applied hydrogen matched the off gas hydrogen flow.

The second part of the cycle was the oxidation reaction performed with steam to generate hydrogen gas. The excess of steam again was condensed in the peltier condenser; the amount of hydrogen produced was detected by the relevant analysis system. No bypass measurements were needed, as only steam was used, which in turn condensed before the analyser. The hydrogen volume flow finally decreased to about zero which indicated the end of the experiment – all of the contact mass should be oxidized at this point. In case of oxidations with synthetic air, as described at the relevant experiment, the end of the reaction could be determined by relating the detected oxygen proportion to the nitrogen proportion. These proportions are constant – 21.0 to 22.5 vol% of oxygen in nitrogen - by using synthetic air. As soon as the oxygen proportion reached the inlet proportion, no further oxidation took place and the experiment was finished. The exact oxygen concentration was determined by reactor bypass measurements.

## 2.4 Synthesis Gas Cycles

To investigate the effects of synthesis gas used for reduction a gas mixture containing hydrogen, carbon monoxide and carbon dioxide was used. A proportion of nitrogen was added to act as internal standard for the analysis system. The *ninth and the tenth experimental series* gave rise to the assumption of side reactions taking place during the reduction with these gas mixtures.

Hydrogen reduces carbon dioxide and forms carbon monoxide and water. Water is condensed and cannot be evaluated; carbon monoxide is a detected product (Equation 17). A small proportion of carbon monoxide is further reduced by hydrogen to methane (Equation 18). As this reaction is the inverted methane reforming reaction, this side reaction is thermodynamically hindered. Carbon monoxide could also be reduced to solid carbon deposits (Equation 19) which in turn can be oxidized during the oxidation step, releasing carbonaceous species as contaminants in the product gas flow (Equation 20 and 21).

$$CO_2 + H_2 \rightarrow CO + H_2O \qquad \Delta H_{298} = +41.2 \text{ kJ/mol} \qquad (17)$$

$$CO + 3H_2 \rightarrow CH_4 + H_2O \qquad \Delta H_{298} = -241.8 \text{ kJ/mol} \qquad (18)$$

$$CO + H_2 \rightarrow C + H_2O \qquad \Delta H_{298} = -153.7 \text{ kJ/mol} \qquad (19)$$

$$C + 2\,H_2O \rightarrow CO_2 + 4\,H_2 \qquad \Delta H_{298} = +90.1 \text{ kJ/mol} \qquad (20)$$

$$C + H_2O \rightarrow CO + H_2 \qquad \Delta H_{298} = +131.3 \text{ kJ/mol} \qquad (21)$$

As there was a constant consumption of hydrogen and carbon dioxide and production of carbon monoxide observable, the side reactions seem to run continuously. These equations could then be used to calculate the appropriate amounts of educts and products from the apparent amounts given by the analysis system.

## 2.5 High Pressure Hydrogen

One of the reasons to investigate the steam-iron process under raised pressure is the over-all efficiency. Producing hydrogen gas and pressurizing it afterwards needs additional equipment and energy. By performing the oxidation of the contact mass, and thus the hydrogen generation under elevated pressure, the additional equipment is not needed – already pressurized hydrogen leaves the reactor system. As part of this work some experiments were performed to investigate the described process. For the oxidations the pressure is limited by the boiling point of water. As pressure increases, the evaporation in the steam generator cannot take place any more. Droplets of water are still transported towards the 600°C hot reactor and the reaction would still take place. The droplets, though reaching the reactor, would then evaporate due to the much higher temperature and react in a non-regular pattern which would make the interpretation of the experiment's results rather difficult due to resulting pressure pulses.

The setup is described in detail under *2.2. Reactor system and analysis.* As the amount of substance was calculated by approximation to an ideal gas, the volume of the test rig's tubing and reactor had to be determined. To achieve this, a predetermined relative pressure of 6.9 bar of hydrogen was set. Then the pressure was decreased by a set volume flow, measuring the time needed and relating it to the pressure difference. By this time duration the test rig's internal volume was calculated; with $p$ for pressure, $V_{gas}$ for the total gas volume at ambient pressure and $V_{MA}$ as the internal volume of MICROACTIVITY (Equation 22).

$$\frac{V_{gas}}{p} = V_{MA} \tag{22}$$

To evaluate the hydrogen generation in the initial period of pressure build-up the previously calculated volume of the test rig's tubing was related to the time to reach the operating pressure of 8 bar. As the apparatus' volume and the maximum pressure were both constant, the amount of generated hydrogen during this period was also constant. The time to reach this pressure and thus this amount of $H_2$ though differed and gave insight into the reactivity of the contact mass. As might be expected, earlier cycles showed higher reactivity than later cycles also in this initial period of the experiments.

# 3 EXPERIMENTAL RESULTS

The experiments were performed in the way described under *Test Procedure*. In case of deviations from this description, the information is given at the relevant position. The diagrams showing the results of reactions offer information on gas conversion as well as gas volume flows. In case of reductions, these volume flows are describing the flow which is converted by the contact mass and thus taken up – low volume flow indicates low amount of reacting gas. In case of oxidation diagrams, the volume flow describes the gases leaving the reactor as products.

## 3.1 Calculations for the result evaluation

To evaluate the results of an experimental series various calculations were necessary. The mass of the used sample was weighed and the amount of reactive contact mass was calculated (Equation 23 – where *m* is the sample mass, *M* the molar mass, *q* the moles of Fe per mole of contact mass, *x* the proportion of Fe – 1 refers to 100 %; *RCM* is the reactive contact mass). These data were used to determine the maximum amount of hydrogen expected to be converted and produced respectively (Equation 24 – where *z* is the oxidation number of iron in the relevant contact mass).

$$\frac{m}{M} * q * 1000 * x = RCM\ [mmol] \tag{23}$$

$$RCM * \frac{z}{2} = max.H_2\ [mmol] \tag{24}$$

The volumetric amount of gas converted is the difference of the inlet stream and the outlet stream. The molar amount is calculated from these values by assuming the condition of ideal gas and a molar volume of 22.4 l/mol. Referring the molar amount of gas either to the contact mass or the expected maximum of hydrogen converted gives additional figures for evaluating the experiments.

Hydrogen and steam conversion were calculated by Equation 25 and Equation 26 respectively. The figure in the result tables is the arithmetic mean of a chosen period of time during the experiment with present gas flows.

$$(1 - \frac{H_{2\ out}}{H_{2\ in}}) * 100 = H_2\ conversion\ [\%] \tag{25}$$

$$(\frac{H_{2\ out}}{H_2O_{\ in}}) * 100 = H_2O\ conversion\ [\%] \tag{26}$$

## 3.2 First experimental series

The first series is separated into several different experiments to understand how to operate the reactions in the test rig and to find out about some crucial test parameters for future experiments. 6.01 g of contact mass V1kl1 (hematite $Fe_2O_3$) was used in this series.

Table 1 shows the amount of contact mass, the reactive proportion and the maximum of possible hydrogen output during reduction.

**Table 1: Contact mass of the 1st series.**

| Contact mass | Contact mass / g | reactive contact mass / mmol | max $H_2$ / mmol |
|---|---|---|---|
| V1kl1 | 6.01 | 75.13 | 112.69 |

### 3.2.1 First and second cycle

In the first and second cycle reduction was performed with 30 ml/min of $H_2$ in a stream of 470 ml/min of $N_2$. As temperature was increased during these cycles from room temperature to operating temperature of 600°C under gas flow, the start of the reaction at about 470°C (after 15 minutes) could be observed (Figure 6 - left). In the second cycle the reduction was accomplished by increasing the hydrogen flow to 60 ml/min (after 140 minutes) for half an hour and then to 100 ml/min (after a total of 170 minutes) to achieve total conversion of the contact mass, even at the price of very low conversion of hydrogen, as depicted in Figure 6 – right.

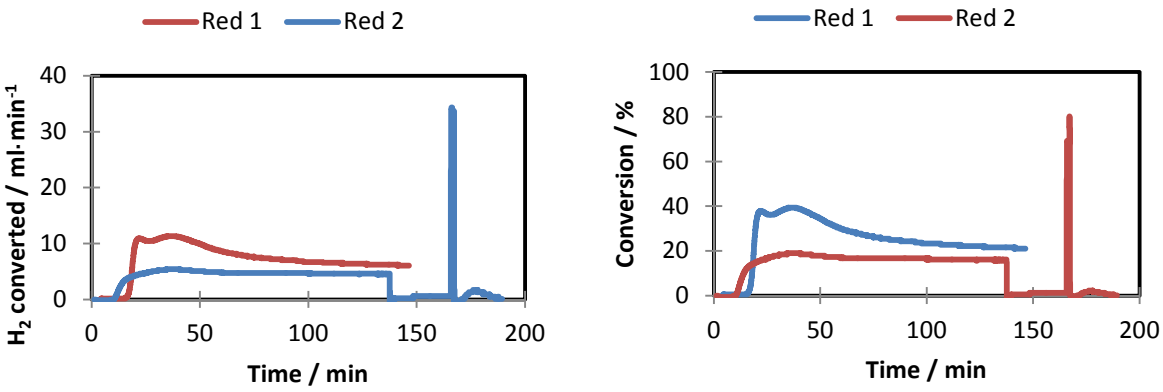


**Figure 6: Hydrogen flow comparison (left) and conversion comparison (right) between 1st and 2nd cycle (1st series).**

At the ends of the two reduction graphs, a difference between the set $H_2$ flow of 30 ml/min and 100 ml/min respectively indicates that there are still reactions occurring, though conversion rates are low, especially in reduction 2. As the reactor's inner diameter is only 0.9 cm and the bed height is about 6 cm, hold-up time is very short (about 0.5 s) at high flows like in these experiments.

Oxidation in the first and second cycle is performed by 0.22 g/min of $H_2O_{(g)}$ in 400 ml/min of $N_2$ for reason of analysis. Conversion rates are rather low, as can be seen in Figure 7 - left. The first oxidation produces also very little hydrogen (Figure 7 – right).

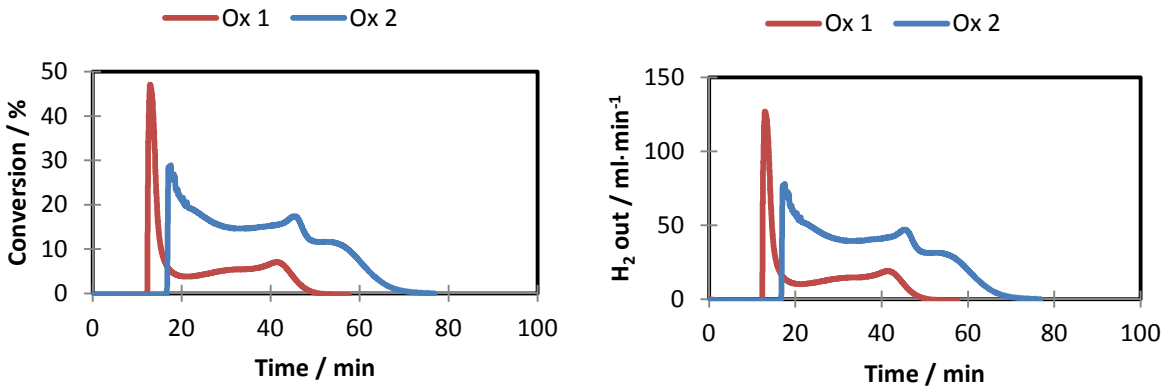


**Figure 7: Steam conversion comparison (left) and hydrogen production (right) between 1st and 2nd cycle (1st series).**

### 3.2.2 Third cycle

In the third redox cycle reduction parameters were investigated more closely – different gas mixtures were analysed by micro GC during the reduction. To oxidize the contact mass, an increasing amount of steam in a medium nitrogen proportion was applied.

In the first part, 5 ml/min of $H_2$ were used in 495 ml/min of $N_2$. The nitrogen stream was changed four times to investigate the influence of the nitrogen proportion on the conversion rate. From minute 64 to 69, 404 ml/min of nitrogen were used. Afterwards the $N_2$ stream was increased to 587 ml/min for five minutes. For another five minutes 678 ml/min of $N_2$ were used as carrier gas, afterwards the original amount of nitrogen was again applied.

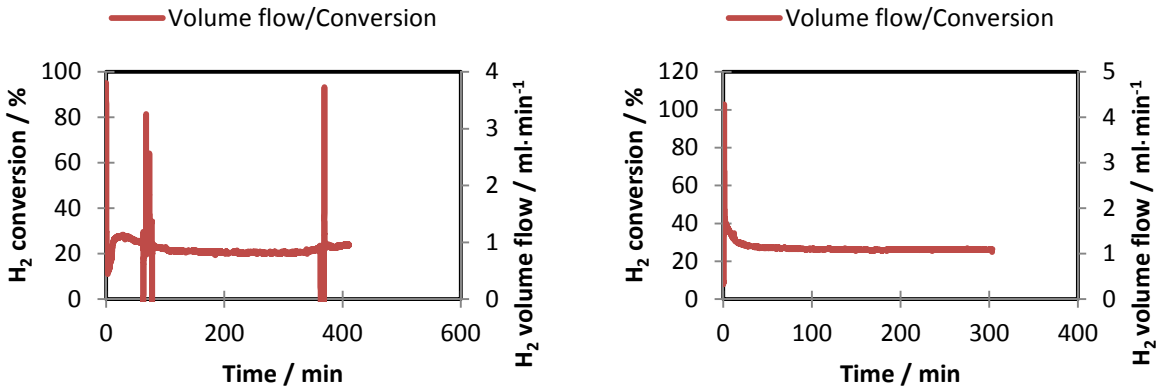


**Figure 8: Reduction of 3rd cycle, part 1 start (left) and finalization (right) (1st series).**

Figure 8 – left shows the change of conversion rate in the first part. Conversion increased when the nitrogen proportion was increased and decreased, when there was less $N_2$ present. The high peaks of 80 or 90 % as well as the 0 % signals derived from operating the mass flow controller. The distortion of the curve at about 370 min is related to a bypass operation to check the reaction progress. Figure 8 – right illustrates the finalization of the reduction, as these data were collected at stable parameters to finish the reduction for a new oxidation step. The amount of consumed hydrogen (Figure 8) did not change for more than 250 minutes, so the experimental part was terminated.

Part 2 continued the experiment with a new test procedure. A total gas flow of 50 ml/min composed of hydrogen and nitrogen was applied. For every 9 minutes (three measurement points) the composition was changed. In between these low flow runs, high flow tests of 5 ml/min of $H_2$ in 490 ml/min of $N_2$ were performed. The low flow tests were done with proportions of 71.6 %, 51.0 %, 30.2 % and 9.6 % of hydrogen.

Comparison between low and high flow experiments clearly shows that conversion is tremendously better at lower gas flows. The proportion of reactive gas at higher hold-up times, thus lower flow rates, does not show much difference, as visible in Table 2.

**Table 2: Conversion rates of various gas mixtures in the 3rd reduction, part 2 (1st series).**

| Mixture | $H_2$ proportion / % | $H_2$ amount / $ml \cdot min^{-1}$ | $N_2$ amount / $ml \cdot min^{-1}$ | Total amount / $ml \cdot min^{-1}$ | $H_2$ conversion / % |
|---|---|---|---|---|---|
| 1 | 71.6 | 35.0 | 13.9 | 48.9 | 19.0 |
| 2 | 51.0 | 25.0 | 24.0 | 49.0 | 20.3 |
| 3 | 30.2 | 14.9 | 34.5 | 49.4 | 19.0 |
| 4 | 9.6 | 4.7 | 44.4 | 49.1 | 21.0 |
| high flow | 1.0 | 5.0 | 490.0 | 495.0 | 11.4 |

In part 3 again various mixtures were examined, where gas flow rates were kept lower than 200 ml/min. For mixtures of all proportions, three to four measurements were made to confirm the arithmetic average of the obtained values. In Table 3 the proportions as well as the resulting conversion rates are displayed. The conversion rate of the end phase is marked by an asterisk to indicate, that no meaningful mean conversion rate could be given as result of rapid decrease of reactivity because of fully reducing the contact mass. The end phase is illustrated in Figure 9.

**Table 3: Conversion rates of various gas mixtures in the 3rd reduction, part 3 (1st series).**

| Mixture | $H_2$ proportion / % | $H_2$ amount / $ml \cdot min^{-1}$ | $N_2$ amount / $ml \cdot min^{-1}$ | Total amount / $ml \cdot min^{-1}$ | $H_2$ conversion / % |
|---|---|---|---|---|---|
| 1 | 71.7 | 35.0 | 13.8 | 48.8 | 21.3 |
| 2 | 4.7 | 4.7 | 95.4 | 100.1 | 20.7 |
| 3 | 1.6 | 4.7 | 297.3 | 302.0 | 16.0 |
| 4 | 2.3 | 4.7 | 196.6 | 201.3 | 18.0 |
| 5 | 9.8 | 9.8 | 90.1 | 99.9 | 15.7 |
| 6 | 14.9 | 14.9 | 85.1 | 100.0 | 14.7 |
| 7 | 19.8 | 19.8 | 80.0 | 99.8 | 13.5 |
| 8 | 25.0 | 25.0 | 74.9 | 99.9 | 14.3 |
| 9 | 71.6 | 35.1 | 13.9 | 49.0 | 18.4 |
| 10 | 2.7 | 4.7 | 169.7 | 174.4 | 22.4 |
| 11 | 4.7 | 4.7 | 95.1 | 99.8 | 21.4 |
| 12 | 24.9 | 24.9 | 75.0 | 99.9 | 13.4 |
| 13 | 30.0 | 30.0 | 70.0 | 100.0 | 13.2 |
| 14 | 35.1 | 35.1 | 64.9 | 100.0 | 13.7 |
| 15 | 40.3 | 40.2 | 59.6 | 99.8 | 13.3 |

| | | | | | |
|---|---|---|---|---|---|
| 16 | 45.3 | 45.1 | 54.5 | 99.6 | 13.6 |
| 17 | 50.5 | 50.3 | 49.3 | 99.6 | 14.3 |
| 18 | 55.1 | 55.0 | 44.9 | 99.9 | 12.3 |
| 19 | 71.8 | 35.2 | 13.8 | 49.0 | 18.2 |
| 20 | 42.1 | 24.8 | 34.1 | 58.9 | 11.7 |
| 21 | 59.3 | 35.1 | 24.1 | 59.2 | 14.4 |
| 22 | 76.4 | 45.1 | 13.9 | 59.0 | 15.3 |
| end phase | 71.8 | 35.1 | 13.8 | 48.9 | * |

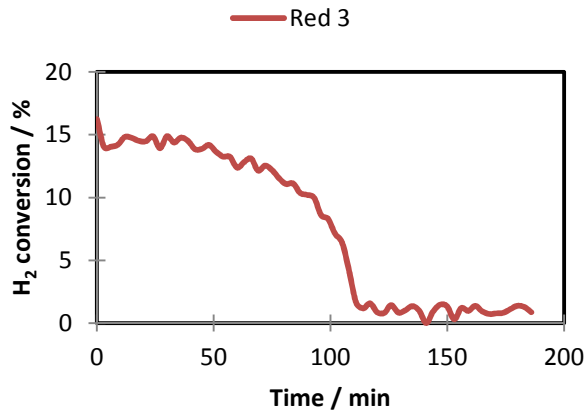


**Figure 9: Hydrogen conversion during the 3rd cycle, part 3 end phase (1st series).**

The oxidation step was performed with an initial amount of 0.008 g/min of steam, which was increased during the end phase to 5.05 g/min for ten minutes and then to 0.08 g/min to finish the experiment. A nitrogen stream of 13.8 ml/min was added as internal standard for gas chromatographic analysis.

Figure 10 shows a high conversion of steam and a conversion drop to almost zero within about 50 minutes. The increase of steam flow is barely visible because it took place after 300 minutes. Figure 10 shows that even an oxidant increase by the factor of 10 could not generate more hydrogen, as the contact mass was already fully oxidized.

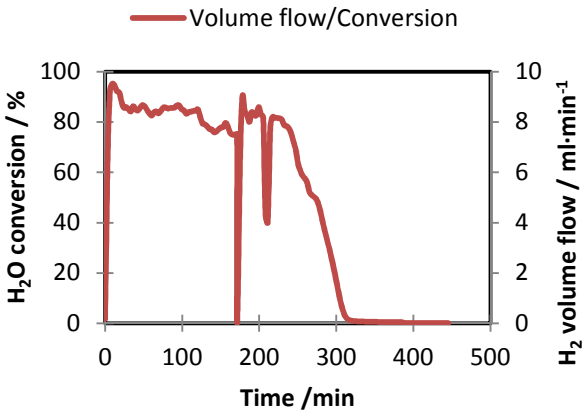


**Figure 10: Oxidation the 3rd cycle (1st series)**

The drop of conversion and $H_2$ flow at about 180 minutes derived from interruption of the experiment whereas the drop at 200 minutes most certainly appeared because of a droplet of water preventing steam flux for some minutes.

### 3.2.3 Fourth cycle

In the fourth cycle parameters were mostly held constant. During reduction a gas mixture of the 3rd cycle with high conversion and low flux was replicated, thus a relatively high hold-up time was achieved accordingly. During oxidation the steam amount was raised for several minutes before returning to standard parameters and raised once again to finish the operation.

During reduction a hydrogen stream of 35.2 ml/min in 13.8 ml/min of nitrogen was used at a temperature of 600°C. The experiment was kept operational for more than 20 hours to reach maximum conversion of the contact mass, recognizable by no remaining hydrogen conversion. As visible in Figure 11 – left, the conversion and thus the amount of converted hydrogen decreases rather rapidly, though conversion never reaches zero. The steep drop at the beginning of the graph at about 85 minutes is only one distorted data point derived from continuation of the experiment after interruption.

In the oxidation step 0.008 g/min of steam were supplied in 13.8 ml/min of nitrogen to re-oxidize the contact mass. During the declining of the conversion the steam flow was increased to 0.08 g/min for 9 minutes (tree data points). After that, the original gas flow was used again. The last 30 minutes (10 data points) again were taken at a raised flow of 0.08 g/min of steam in 13.8 ml/min of nitrogen.

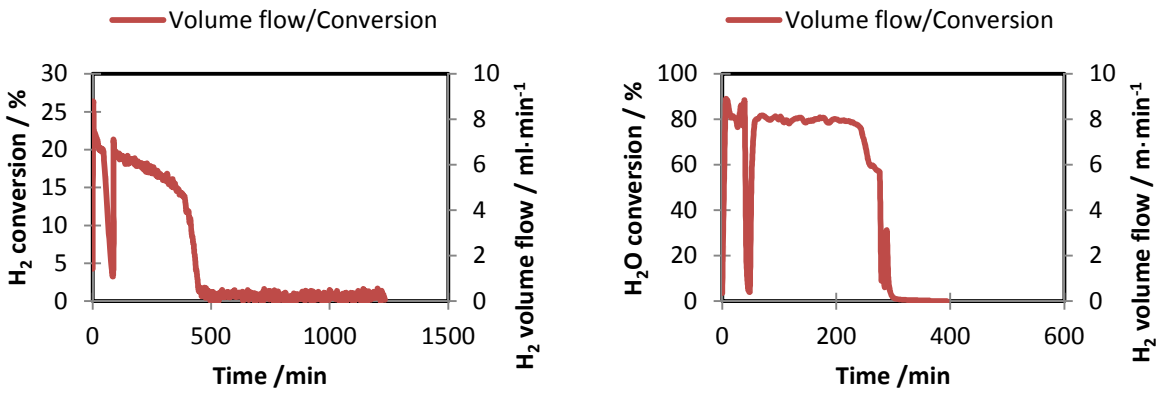


**Figure 11: Reduction (left) and oxidation (right) of the 4th cycle (1st series)**

As expected, conversion did not increase over the nine minutes of high steam flow at about 280 minutes (Figure 11 – right). A steep increase is followed by a sharp drop. The second increase of steam flow did not raise the amount of produced hydrogen, as the contact mass already was fully oxidized (Figure 11 – right – 365 minutes to the end). At about 50 minutes minor system instability caused distorted measurement signals.

### 3.2.4 Fifth cycle

Parameters were held constant in this experiment. The reduction reaction was performed under the same conditions as before. For the oxidation reaction water supply was performed with a HPLC pump and the reactor was operated under pressure.

The reduction of the 5$^{th}$ cycle was carried out again at 600°C with a $H_2$ stream of 35.2 ml/min in 13.8 ml/min of $N_2$. As seen in Figure 12 – left, the initially higher conversion of about 28 % drops fast as the contact mass proportion of the highest oxidation state is reduced. Continuous diminishing of conversion is observable throughout the experiment, though three areas could be identified.

The first area is the area of the steepest drop, from zero to about 30 minutes. Between 30 and 300 minutes the second area is located. The third area can be defined from 300 to approximately 410 minutes. Each of these areas could identify changes of oxidation state in the contact mass.

Again no baseline of zero hydrogen conversion could be obtained; some reactions were still going on even after 900 minutes of continuous operation.

The first oxidation under raised pressure was performed with a $H_2O_{(g)}$ stream of 0.07 g/min in 13.8 ml/min of $N_2$ at 600°C. Pressure was built up in the reactor by use of a needle valve included in the test rig. As soon as the defined pressure of 3.0 bar was reached, the valve's regulator switched. Thus a steep flow increase is visible in Figure 12 – right, at the beginning.

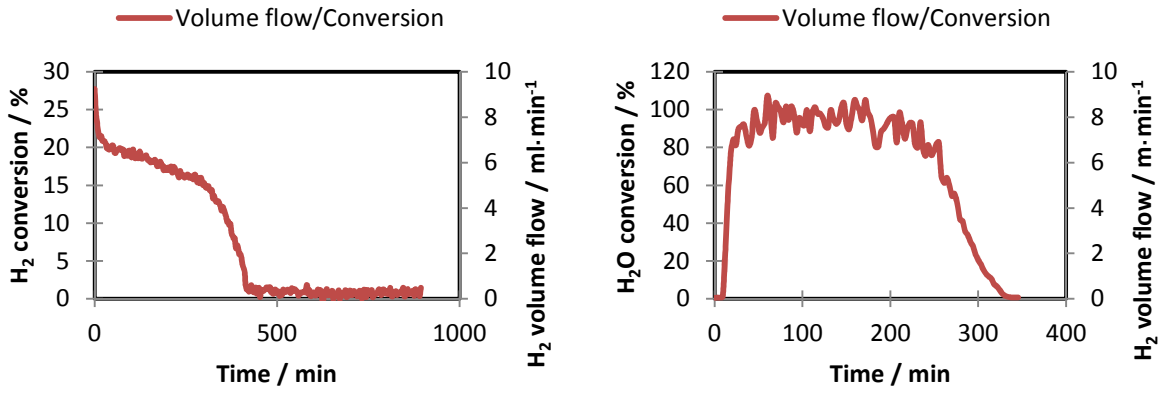


**Figure 12: Reduction (left) and oxidation (right) of the 5$^{th}$ cycle (1$^{st}$ series).**

By pulsation caused by the PID regulator of the needle valve, gas flow as well as conversion is not as stable as in previous experiments. This pulsation is also the reason for apparent conversion rates higher than 100 % (Figure 12 - right).

### 3.2.5 Sixth cycle

The last cycle of this series in fact consists only of a reduction, as water supply problems prevented the oxidation step. For reduction a stream of 35.2 ml/min of $H_2$ in 13.8 ml/min of $N_2$ was used at 600°C.

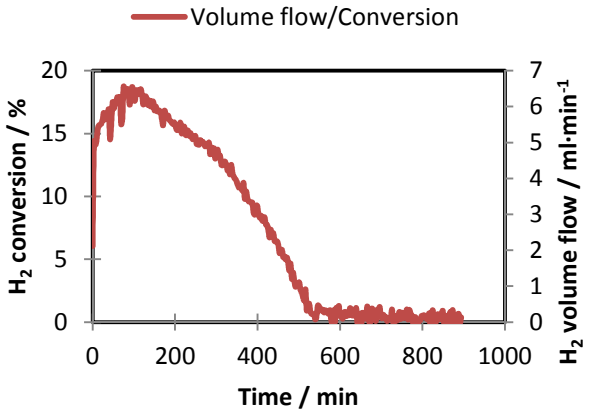


**Figure 13: Reduction of the 6th cycle (1st series).**

The increase of conversion up to a maximum of about 18 %, which is in fact lower than the starting conversion of the previous cycle could possibly indicate advanced degradation of the contact mass. The conversion in Table 4 was calculated from the beginning to 535 minutes, to "cut off" the very low flux area.

### 3.2.6 Results

Table 4 offers the relevant data for the performed series. Conversion is calculated in set parts, where gas flow was still present. The next to last column ($H_2$ / mmol·$g^{-1}$) indicates the amount of hydrogen in relation to the total contact mass. The obtained data does not fit together neatly as experimental parameters are changed in nearly every cycle. It is obvious that the experiments of the 4$^{th}$, 5$^{th}$ and 6$^{th}$ cycle converted the contact mass to a higher extent. This gives rise to the assumption that these reactions were carried out in a much more complete way than earlier experiments.

**Table 4: Results of the 1$^{st}$ series.**

| Reaction | $H_2$ / mmol | $H_2$ / ml | $H_2$ conversion / % | $H_2O$ conversion / % | $H_2$ / mmol·$g^{-1}$ | Contact mass conversion / % |
|---|---|---|---|---|---|---|
| Reduction 1 | 50.40 | 1128.98 | 26.75 | - | 8.39 | 44.73 |
| Oxidation 1 | 30.51 | 683.45 | - | 4.40 | 5.08 | 27.07 |
| Reduction 2 | 70.29 | 1574.41 | 7.22 | - | 11.70 | 62.38 |
| Oxidation 2 | 82.99 | 1858.87 | - | 12.42 | 13.81 | 73.65 |
| Reduction 3 | 47.39 | 1061.58 | * | - | 7.89 | 42.05 |
| Oxidation 3 | 97.84 | 2191.72 | - | 70.38 | 16.28 | 86.82 |
| Reduction 4 | 106.02 | 2374.89 | 14.99 | - | 17.64 | 94.08 |
| Oxidation 4 | 94.01 | 2105.88 | - | 55.82 | 15.64 | 83.43 |
| Reduction 5 | 105.98 | 2373.84 | 16.04 | - | 17.63 | 94.05 |
| Oxidation 5 | 96.21 | 2155.17 | - | 71.31 | 16.01 | 85.38 |
| Reduction 6 | 103.70 | 2322.94 | 12.35 | - | 17.25 | 92.02 |

Hydrogen uptake in reductions and yield in oxidation in the first two cycles differ because of termination of the reaction at different times as the goal for these cycles was to find just parameters for next experiments.

For the reduction of the third cycle conversion is marked by an asterisk, as there are different conversion rates in this experiment to look up further above.

## 3.3 Second experimental series

In the second series various experimental parameters such as pressure and temperature were changed. For hydrogen production under pressure, water was supplied by a HPLC pump. Contact mass was sponge iron impregnated with 5 wt% of aluminium oxide. Table 5 offers the relevant data for the current series.

**Table 5: Contact mass of the 2nd series.**

| Contact mass | Contact mass / g | reactive contact mass / mmol | max $H_2$ / mmol |
|---|---|---|---|
| $Fe/Al_2O_3$ 5 wt% | 6.30 | 107.16 | 142.88 |

### 3.3.1 First cycle

The parameters for the first reduction are similar to the experiments before – 40.2 ml/min of hydrogen and 14.1 ml/min of nitrogen act as reducing gas mixture for the contact mass. As the gas flow was turned on during the running GC system, the initial increase of converted gas and conversion respectively, are related to an increase of reacting gas (Figure 14 – left). This seems not to be related to a chemical reaction.

After a short period of high conversion, continuous decrease of conversion was observable. The reason for the high conversion is related to the high oxidation state of parts of the contact mass due to sample preparation at 900°C under atmospheric conditions. A gas pulse because of switching the mass flow controllers probably adds to this effect. As there are no periods of constant conversion, hold up time seems to be insufficient. Compared to the last cycles of the previous series, higher conversion is visible due to a new contact mass.

As a preliminary experiment for chemical looping combustion, the oxidation was done with synthetic air. The nitrogen proportion of the synthetic air acts as internal standard for the analysis system in this case, so the conversion of the oxygen proportion can be displayed in Figure 14 – right.

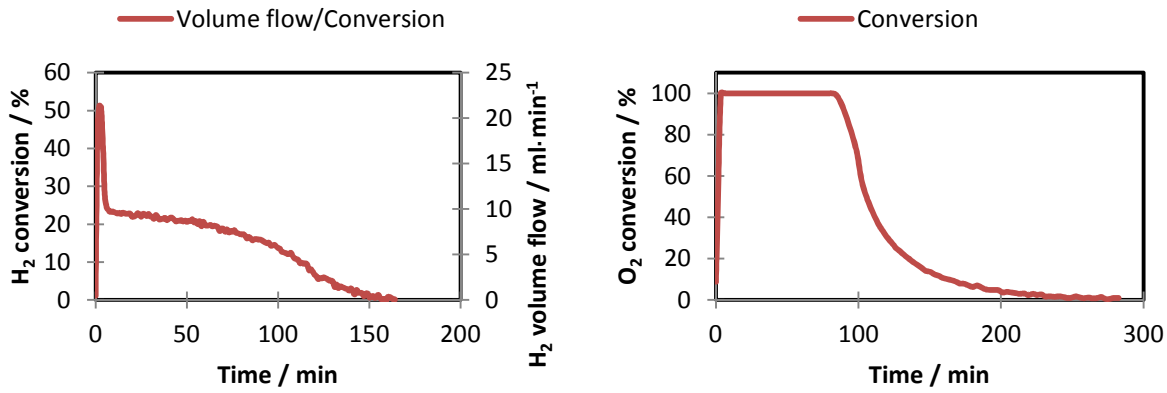


**Figure 14: Reduction (left) and oxidation (right) of the 1st cycle (2nd series).**

The conversion is about 100 % for some 80 minutes. Then a rapid decrease of conversion indicates a very efficient oxidation. The increase at the beginning again is related to starting the gas flow.

### 3.3.2 Second cycle

The reduction was tested with methane in nitrogen but had to be terminated prematurely because of fast pressure increase due to carbon deposition on the contact mass. A stream of 19.9 ml/min of $CH_4$ was added to 13.8 ml/min of $N_2$ to reduce the $Fe/Al_2O_3$ 5 wt% at a temperature of 750°C (Equation 27). When pressure reached 5 bar, the experiment was stopped.

The initial steep peak in Figure 15 – left again is partly related to the previously mentioned "gas pulse" by starting the flows. It seems to take quite a while (120 minutes) to reach maximum conversion of greater than 95 %. As there are also other gases present during the reaction various side reactions are possible, as Figure 15 indicates.

Initially there are only iron oxides present in the reactor – methane is used up to reduce this species. After having reduced a critical amount to metallic iron, this species could act in a catalytic way to split methane [31].

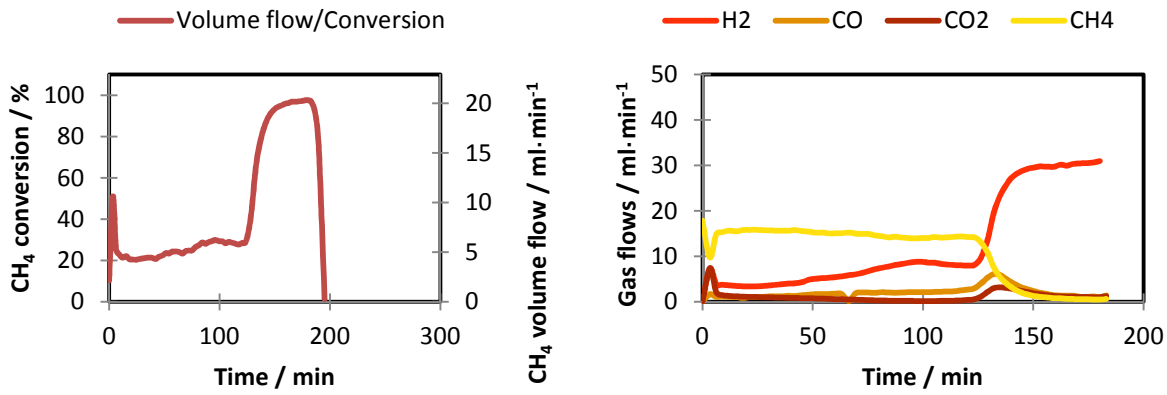


**Figure 15: Conversion of methane (left) and gas flows of all relevant gases in reduction (right) of the 2nd cycle (2nd series).**

Hydrogen most certainly was produced by thermal decomposition of methane forming coke, as shown in Equation 27, which then resulted in the raising pressure in the reactor by plugging the gas flow. The proportion of decomposed $CH_4$ (degree of splitting) was calculated with the thermodynamics software Aspen Plus and is shown in Figure 16 as a function of temperature.

$$CH_4 \rightarrow C + 2\,H_2 \qquad \Delta H_{298} = +73.4 \text{ kJ/mol} \qquad (27)$$

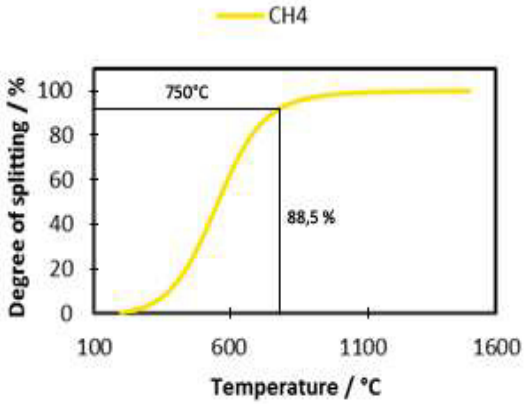


**Figure 16: Splitting of Methane as function of the temperature – calculated with Aspen Plus.**

As the only oxygen source is the iron oxide, the formed carbon reacts with the oxides to further reduce them until there is no oxygen left. Then solid carbon is deposited on the contact mass, as gaseous compounds like CO or $CO_2$ cannot be generated any more.

The following oxidation done with synthetic air was started with low flows of 8.5 ml/min, as the coke plug was too tight to allow higher flows. After 126 minutes the gas flow was increased to 20.1 and after the next 30 minutes to 50.4 ml/min of syn air. Changing the oxidant flow is also visible in Figure 17.

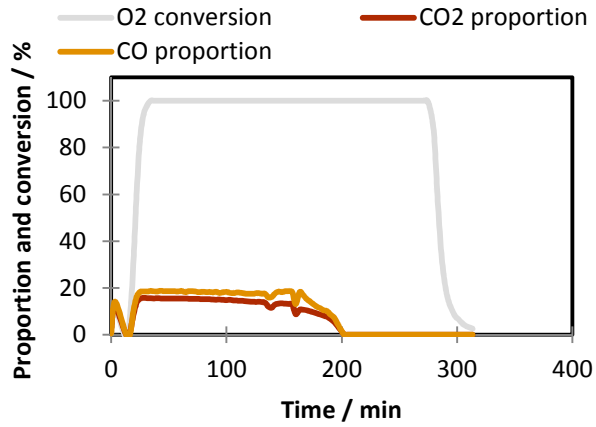


**Figure 17: Oxygen conversion and carbonaceous species of the 2nd cycle (2nd series).**

High conversion of oxygen and a rapid decrease in conversion both indicate a full oxidation of the contact mass to hematite. The diminishing proportion of both predominant carbonaceous species – $CO_2$ and CO – formed during oxidation clearly shows the liberation of the contact mass of contaminating carbon.

### 3.3.3 Third cycle

The third cycle again was performed with hydrogen as reductive gas and steam as oxidant. The needle valve of the test rig was set corresponding to 10 bar relative pressure. Pressure increase was forced by the steam/nitrogen flow applied.

For reduction a $H_2$ flow of 35.2 ml/min in 13.8 ml/min of $N_2$ was used at 600°C. As usual, the reduction was not performed at raised pressure.

Figure 18 – left displays the conversion of $H_2$ and the corresponding volume flow. High conversion due to the high state of oxidation at the beginning (hematite $Fe_2O_3$ by oxidation with oxygen in the previous oxidation step) is followed by rather low and constantly decreasing conversion rates. This low conversion possibly relates to the degradation of the contact mass, as the last cycle was more stressful than others. Higher temperatures and the highly exothermic oxidation with air could have damaged the contact mass.

During the oxidation the gas flows were set and the needle valve opened at a defined relative pressure of 10 bar. At the end of the reaction (420 min), steam was increased from 0.008 g/min of steam to 0.08 g/min.

Constant high conversion during the reaction and a steep decrease at the end indicates good performance at raised pressure. The fact, that conversion is lower than in the first cycle at raised pressure is related to degradation of the contact mass possibly related to loss of active surface. Again pulsation was observable, as the PID regulator was working to keep the pressure constant over varying flow.

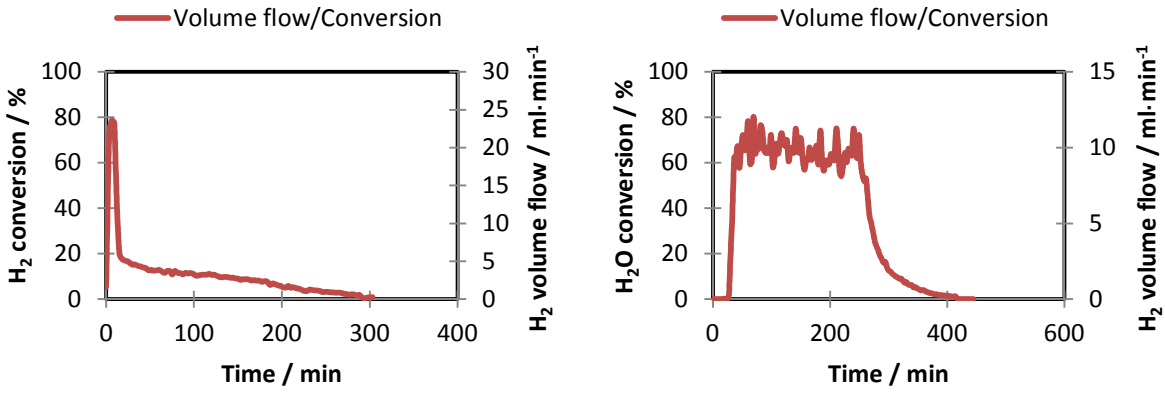


**Figure 18: Reduction (left) and oxidation (right) of the 3rd cycle (2nd series).**

### 3.3.4 Fourth cycle

Gas flows of the 4th cycle of this series are nearly the same as in the 3rd cycle – 35.2 ml/min of H2 and 13.8 ml/min of N2 in reduction but 0.01 g/min of $H_2O_{(g)}$ in oxidation. Temperature was changed from 600°C to 750°C for both reactions. Though the oxidation is an exothermic reaction, the higher temperature was picked for this reaction as well, in order to investigate if cooling the reactor between these steps was necessary.

During the reduction, the hydrogen flow was increased to 70.7 ml/min after 255 minutes to finish the step. In Figure 19 – left, a decrease of conversion from a high starting point to a

kind of stable plateau of about 30 % conversion followed by another drop is shown. This refers to the oxidation state of wuestite (FeO). The highest conversion occurs at the presence of magnetite ($Fe_3O_4$). Due to the high conversion and the fact that reducing $Fe_3O_4$ yields three times the amount of FeO per mole of $H_2$, this step is much faster than the following step from FeO to metallic iron.

Temperature for the oxidation was set at 750°C and pressure limited at 10 bar. The steam flow was started at 0.008 g/min and increased to 0.8 g/min after 363 minutes for finishing the oxidation.

Similar to the previous experiment with a pressurized reactor, the sharp drop of $H_2$ flow indicates the end of the reaction. To achieve a total conversion of the contact mass, steam was added in excess (Figure 19 – 363 minutes). Though the amount of hydrogen increases, the conversion drops to about zero. As the reaction is going at very low efficiency, the contact mass is considered converted to magnetite $Fe_3O_4$.

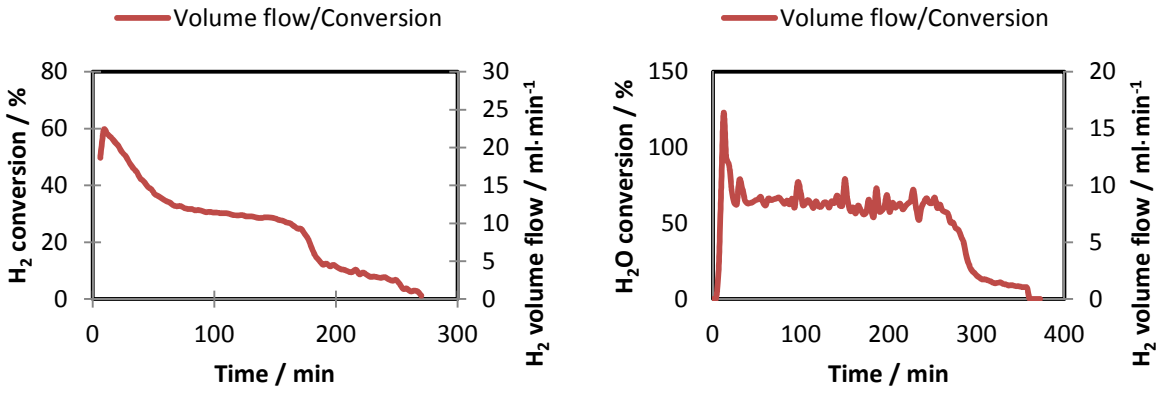


**Figure 19: Reduction (left) and oxidation (right) of the 4th cycle (2nd series).**

### 3.3.5 Results

**Table 6: Results of the 2nd series.**

| Reaction | $H_2$ / mmol | $H_2$ / ml | $H_2$ conversion / % | $H_2O$ conversion / % | $H_2$ / mmol·$g^{-1}$ | Contact mass conversion / % |
|---|---|---|---|---|---|---|
| Reduction 1 | 133.10 | 2981.51 | 14.68 | - | 21.13 | 93.16 |
| Oxidation 1 | - | - | - | * | - | * |
| Reduction 2 | - | - | - | - | - | - |
| Oxidation 2 | - | - | - | - | - | - |
| Reduction 3 | 50.12 | 1122.77 | 10.98 | - | 7.96 | 35.08 |
| Oxidation 3 | 109.49 | 2452.48 | - | 42.46 | 17.38 | 76.63 |
| Reduction 4 | 132.34 | 2964.36 | 25.63 | - | 21.01 | 92.62 |
| Oxidation 4 | 125.2 | 2804.44 | - | 50.66 | 19.87 | 87.62 |

As the first and the second cycle were designated preliminary experiments, the obtained data is not comparable with the third and the fourth cycle (Table 6). The difference in reduction and oxidation in the third cycle is more than 50 % of converted and generated hydrogen respectively. This possibly happened because of incomplete previous experiments. The fourth reduction and oxidation fit together better, which indicates completeness of the respective reactions in the cycle.

## 3.4 Third experimental series

### 3.4.1 First cycle

For the third series an alternative analysis system was applied – a red-y mass flow controller (Vögtlin, Switzerland) was installed at the gas outlet and used to measure the hydrogen flow in the way of a mass flow meter. 6.04 g of contact mass $Fe/Al_2O_3$ 5 wt% - sponge iron impregnated with aluminium oxide (Table 7) was used in this series.

**Table 7: Contact mass of the 3rd series.**

| Contact mass | Contact mass / g | reactive contact mass / mmol | max $H_2$ / mmol |
|---|---|---|---|
| $Fe/Al_2O_3$ 5 wt% | 6.04 | 102.79 | 137.05 |

The reduction reactions were carried out at a temperature of 750°C and a gas flow of 35 ml/min of hydrogen. As the reaction was started with the highly oxidized species of hematite, initially high rates of conversion were possible. The high conversion at the beginning (Figure 20) is not followed by a clearly visible magnetite phase. Instead the wuestite period at about 30 % is prominent. After the last drop of reactivity to metallic iron, at about 240 minutes the gas flow was increased to 75 ml/min.

For the oxidation step, a gas flow of 0.04 g/min of steam was applied at 600°C. After 90 minutes, the steam flow was increased to 0.36 g/min. As the oxidation was carried out at raised pressure, 10 bar were set via the test rig's internal pressure regulator.

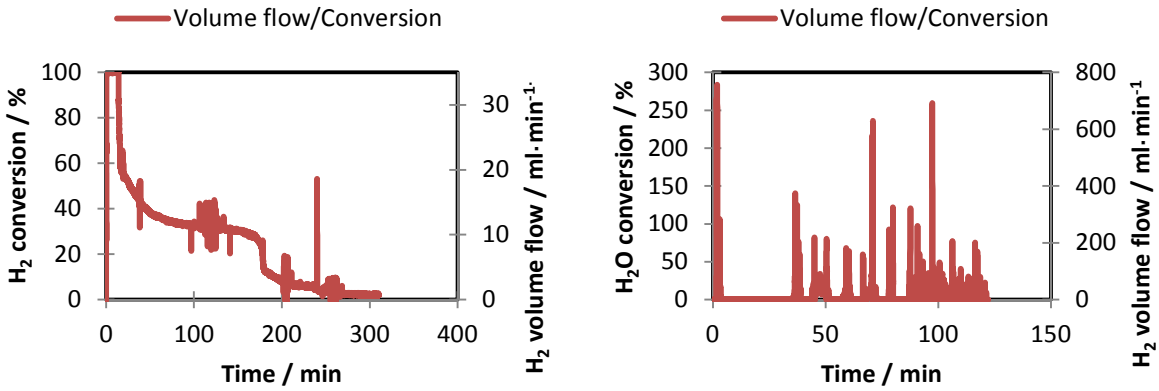


**Figure 20: Reduction (left) and oxidation (right) of the 1st cycle (3rd series).**

As displayed in Figure 20 – right, the volume flow during the experiment was inconsistent due to the regulation delay of the PID regulator. An initial flow occurred because of the not yet fully closed MFC, then the pressure build-up took about 30 minutes – no flow was observable. Because there is no inert gas like nitrogen present, the product gas flow consists only of hydrogen. As this stream is dependent of conversion and pump characteristics, a pulsation can occur, which leads to pulsation of the regulator. Combined with the regulating delay, this is further amplified by either closing or opening the needle valve too much.

### 3.4.2 Second cycle

The reduction parameters were kept the same as in the first cycle – 35 ml/min of $H_2$ at 750°C. The reduction (Figure 21 – left) starts at an initial conversion rate of about 40 %, which is not representative for a reduction of magnetite $Fe_3O_4$ with $H_2$. Also, a low total amount of converted hydrogen is a sign for an incomplete previous cycle.

During the oxidation (Figure 21 – right) a steam flow of 0.04 g/min was used. At 600°C and 9 bar pressure, the reaction was carried out without any nitrogen. An inconsistent flow was observable, mainly because of the needle valve regulator's delay.

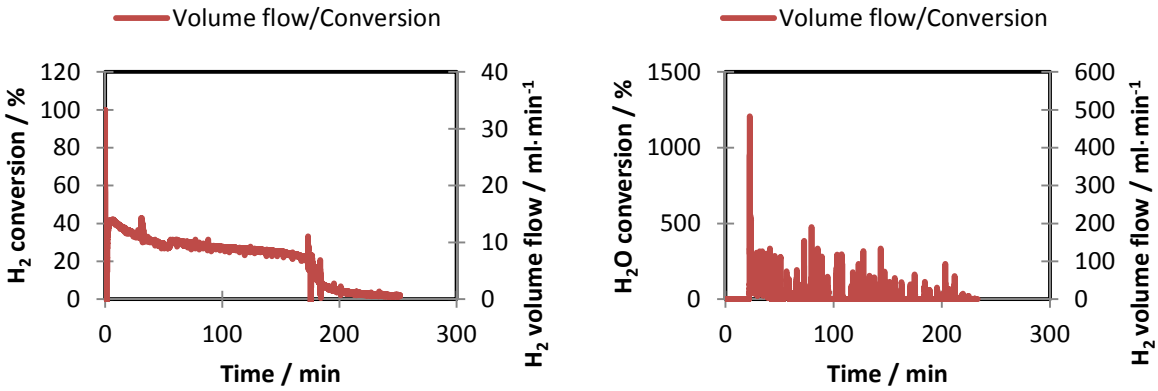


**Figure 21: Reduction (left) and oxidation (right) of the 2nd cycle (3rd series).**

### 3.4.3 Third cycle

The cycle was performed with 39.8 ml/min of $H_2$ at 750°C for reducing and 0.04 g/min of $H_2O_{(g)}$ at 600°C in the oxidation step. Figure 22 – left shows a start of the reaction at conversion rates lower than 60 %, which indicates a low oxidation state of the contact mass. The magnetite proportion seems to be hardly present.

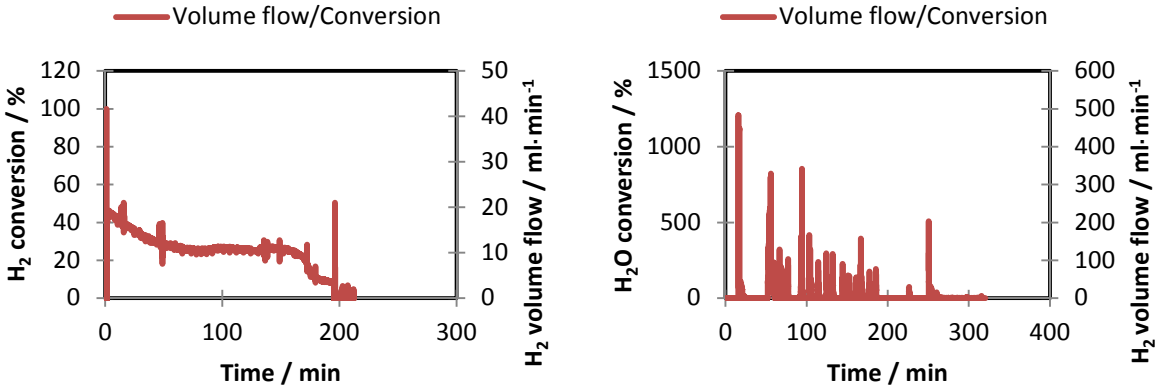


**Figure 22: Reduction (left) and oxidation (right) of the 3rd cycle (3rd series).**

As shown in the previous cycle, an inconsistent product gas stream in the oxidation step (Figure 22 – right) related to the needle valve was present in this cycle. The amount of hydrogen set free in every 100 minutes interval of the oxidation is shown in Figure 23. This gives an impression of the very intense reaction mainly at the beginning.

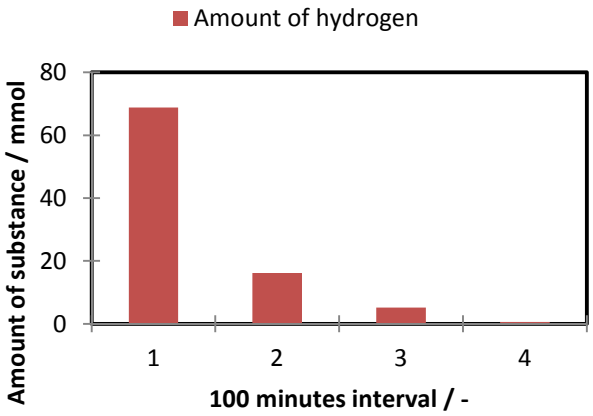


**Figure 23: Produced hydrogen during the oxidation of the 3rd cycle (3rd series).**

### 3.4.4 Fourth cycle

The reduction was carried out at 750°C with 39.8 ml/min of hydrogen, the gas flow was increased to 70 ml/min after 210 minutes to drive the reaction to the end. As visible in Figure 24 – left, there is a flow of hydrogen present when the reaction was terminated.

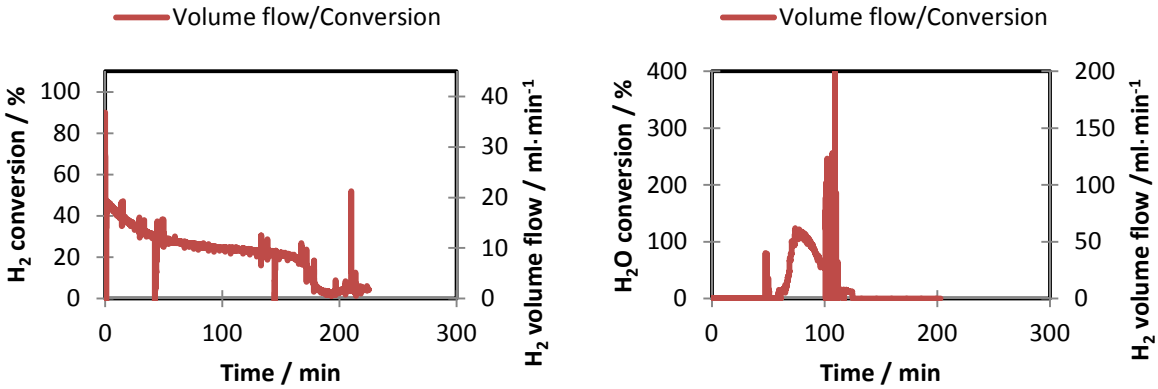


**Figure 24: Reduction (left) and oxidation (right) of the 4th cycle (3rd series).**

The oxidation of this cycle was carried out under increased pressure manually set via the needle valve of the test rig. As this was some kind of test to keep the flow at a constant level, the results are not quite representative.

### 3.4.5 Results

Table 8 displays the results of the series and indicates that the oxidation of the first cycle was not performed until complete oxidation of the contact mass. Related to the hydrogen converted in the reduction, the oxidation released just about a fifth of the amount. For the second cycle, about twice as much hydrogen is generated compared to the used up $H_2$. In the previous cycle the contact mass was not completely oxidized, in the second cycle though, significantly more hydrogen was produced. The fact that the produced amount nearly doubles the amount of $H_2$ used up derives from the incomplete first cycle. Comparison between the reduction and oxidation of the third cycle shows that the experiments fit together tightly – the amount of used up hydrogen nearly equals the amount produced during the oxidation. The difference most certainly is related to error in measurement of the mass flow controller.

**Table 8: Results of the 3rd series.**

| Reaction | $H_2$ / mmol | $H_2$ / ml | $H_2$ conversion / % | $H_2O$ conversion / % | $H_2$ / mmol·g$^{-1}$ | Contact mass conversion / % |
|---|---|---|---|---|---|---|
| Reduction 1 | 127.35 | 2852.74 | 25.52 | - | 21.07 | 92.92 |
| Oxidation 1 | 25.12 | 562.76 | - | 10.32 | 4.16 | 18.33 |
| Reduction 2 | 44.84 | 1004.36 | 18.92 | - | 7.42 | - |
| Oxidation 2 | 89.60 | 2007.08 | - | 19.11 | 14.83 | - |
| Reduction 3 | 88.49 | 1982.26 | 23.43 | - | 14.64 | 64.57 |
| Oxidation 3 | 90.70 | 2031.68 | - | 13.85 | 15.01 | 66.18 |
| Reduction 4 | 61.43 | 1375.97 | 15.37 | - | 10.17 | 44.82 |
| Oxidation 4 | 73.71 | 1651.18 | - | 57.81 | 12.20 | 53.78 |

## 3.5 Fourth experimental series

The freshly prepared contact mass *Fe/$Al_2O_3$ 5%* was applied for this series (Table 9). All reduction steps were carried out at the same conditions – 35 ml/min of hydrogen were used at 750°C and ambient pressure. In the oxidation steps, 0.04 g/min of steam were used at 750 °C and raised pressure. Pressure control was performed automatically by a PID controller regulating the test rig's needle valve.

**Table 9: Contact mass of the 4th cycle.**

| Contact mass | Contact mass / g | reactive contact mass / mmol | max $H_2$ / mmol |
|---|---|---|---|
| Fe/$Al_2O_3$ 5 wt% | 6.52 | 110.90 | 147.87 |

### 3.5.1 First cycle

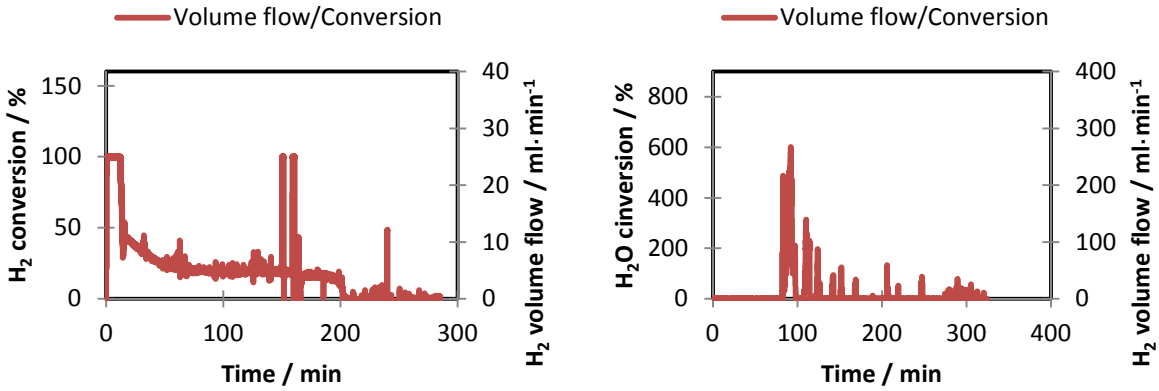


**Figure 25: Reduction (left) and oxidation (right) of the 1st cycle (4th series).**

To finish the reduction, the steam flow was doubled after four hours of reaction (Figure 25 – left, after 240 minutes). This happened after the decrease of reactivity, thus the influence on the reaction was minimal.

The high conversion at the beginning again refers to the reaction with the hematite phase, which is reduced. The two high peaks at 150 and 160 minutes can be related to the manually induced increase in pressure to empty the system's gas-liquid separator.

During the oxidation it took some time to build up the operating pressure of 9 bar, thus no flow until minute 90 was present. After 285 minutes the amount of steam was increased to about 0.36 g/min to achieve total conversion of the contact mass.

### 3.5.2 Second cycle

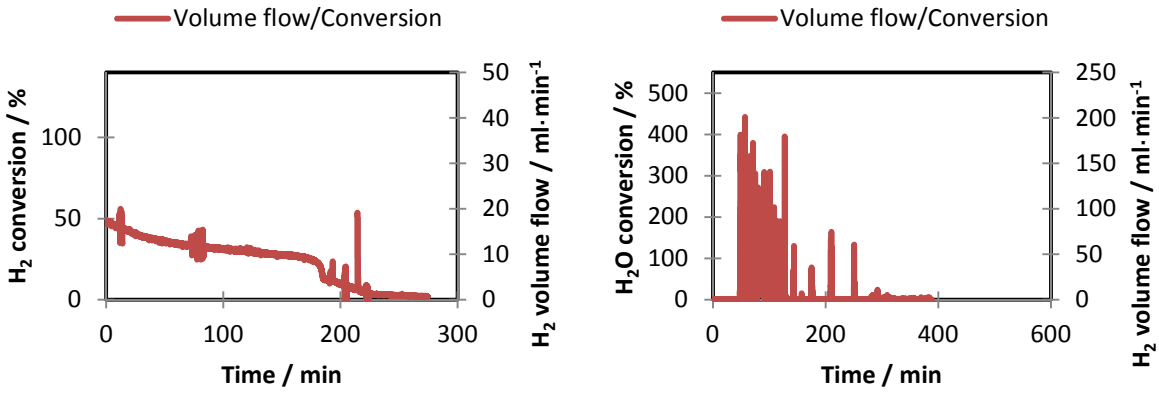


**Figure 26: Reduction (left) and oxidation (right) of the 2nd cycle (4th series).**

At the end of the reduction step, again a higher flow of 70 ml/min of $H_2$ was used. Switching to a higher gas stream is indicated by a peak at 215 minutes. The reduction (Figure 26 – left) took place at much lower conversion rates at the beginning, showing not only the absence of hematite but also a low amount of magnetite in the contact mass, as there is only one step observable. The magnetite step seemed to be too small to be identified independently.

Reoxidising the contact mass at about 9 bar with steam shows the initial high gas yield for about 100 minutes (Figure 26 – right, 50 to 150 minutes). After about 300 minutes experimental time the steam flow was increased to 0.36 g/min to fully oxidize the contact mass for the next cycle.

### 3.5.3 Third cycle

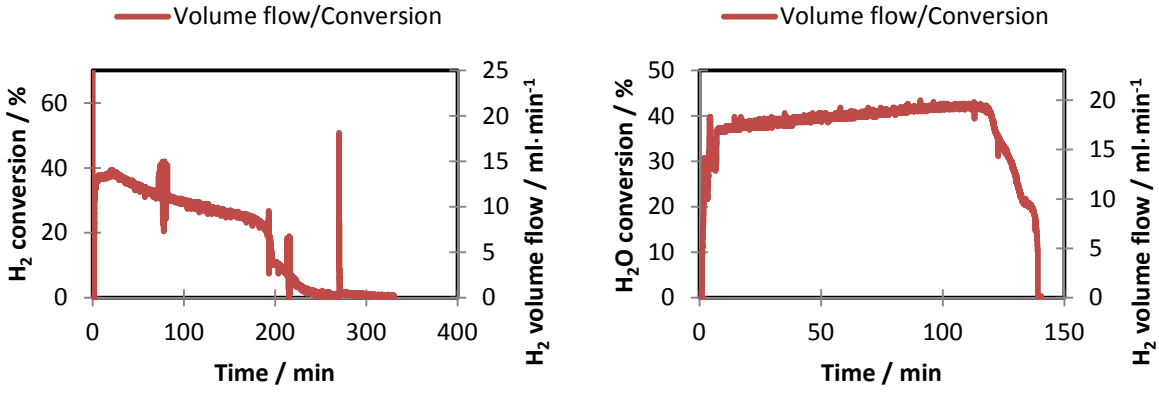


**Figure 27: Reduction (left) and oxidation (right) of the 3rd cycle (4th series).**

Like the previous reductions the reaction was finished by an increased flow of hydrogen at 270 minutes. The gas stream was doubled to 70 ml/min after the reaction was nearly over.

The oxidation (Figure 27 – right) was carried out at ambient pressure. As there is no valve regulating the flow, a constant product gas stream is detected and quantified. After a slow increase of conversion and gas flow the contact mass is oxidized to a high proportion. A decrease in two steps is observable, possibly referring to different oxidation states. Most certainly both oxidation states are present throughout most of the experiment – one outlasts the other.

### 3.5.4 Fourth cycle

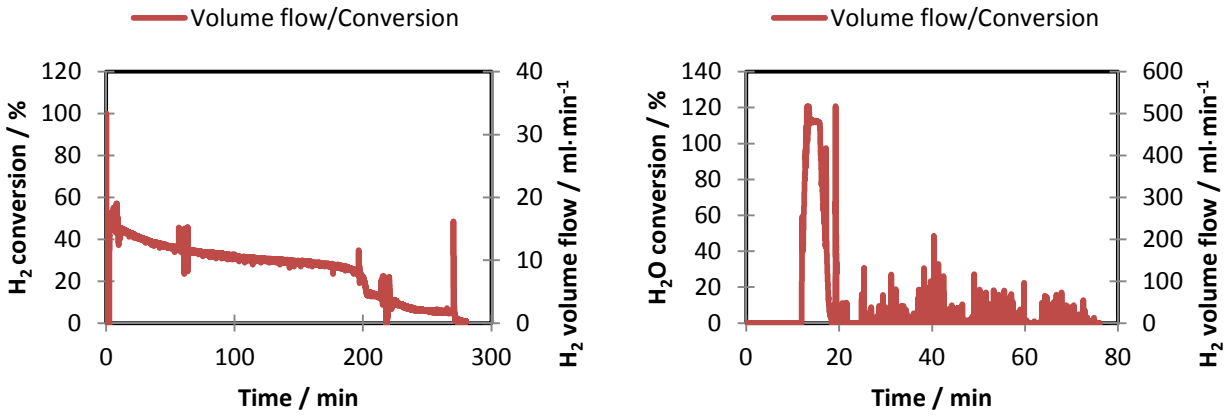


**Figure 28: Reduction (left) and oxidation (right) of the 4th cycle (4th series).**

The reduction was carried out under the previously discussed parameters – 35 ml/min of $H_2$ at 750°C.

As the oxidation was performed with the tenfold amount of steam, which is regularly only used to finish the reaction, a high flow of hydrogen was observable during the time of maximum conversion at the beginning. Due to the higher flow the pressure control system operated much more stable than before. When there was almost no gas flow observable any more, the experimental series was terminated.

### 3.5.5 Results

The amount of generated hydrogen in the first cycle is once again higher than the amount of consumed reductive gas in the previous reduction. This can be explained by a contact mass not fully oxidized during the synthesis, an effect which could be observed quite regularly.
Most interestingly the two reactions of the second cycle perfectly fit together – the amounts of consumed and generated hydrogen are nearly identical, though the conversion during the oxidation is significantly lower. This can be explained by the inconstant gas flow due to the pressure regulating system.

Evaluating the amounts of hydrogen gas converted and produced in the third cycle, the oxidation again seems to yield a slight excess which could be explained by over-detection due to moisture which got into the analysis system. As there is no pressure built up before the mass flow controller, the product gas directly reaches the analyser. The experiment at ambient pressure takes less time than pressure experiments, the gas stream moves faster. This gives rise to the assumption that the hold-up time in the condenser is lower and more moisture reaches the exit of the test rig, leading to the error in measurement.

In the fourth cycle the amounts of gas converted and set free are again comparable.

**Table 10: Results of the 4$^{th}$ series.**

| Reaction | $H_2$ / mmol | $H_2$ / ml | $H_2$ conversion / % | $H_2O$ conversion / % | $H_2$ / mmol·g$^{-1}$ | Contact mass conversion / % |
|---|---|---|---|---|---|---|
| Reduction 1 | 64.05 | 1434.69 | 13.45 | - | 9.82 | 43.31 |
| Oxidation 1 | 100.81 | 2258.25 | - | 18.39 | 15.46 | 68.18 |
| Reduction 2 | 107.23 | 2402.06 | 22.06 | - | 16.45 | 72.52 |
| Oxidation 2 | 107.77 | 2413.98 | - | 13.54 | 16.53 | 72.88 |
| Reduction 3 | 91.33 | 2045.76 | 17.70 | - | 14.01 | 61.76 |
| Oxidation 3 | 100.81 | 2327.46 | - | 31.86 | 15.46 | 68.18 |
| Reduction 4 | 112.51 | 2520.15 | 24.14 | - | 17.26 | 76.08 |
| Oxidation 4 | 113.54 | 2543.39 | - | 8.87 | 17.41 | 76.79 |

## 3.6 Fifth experimental series

The fifth series was carried out with pure sponge iron as contact mass at operational parameters similar to these of the previous series. The relevant data of the contact mass is given in.

**Table 11: Contact mass of the 5th series.**

| Contact mass | Contact mass / g | reactive contact mass / mmol | max $H_2$ / mmol |
|---|---|---|---|
| Fe | 5.54 | 99.27 | 132.36 |

### 3.6.1 First cycle

To start the experimental series with a reduction is some kind of developed praxis, although pure, untreated sponge iron is used and should already be at the lowest possible oxidation state.

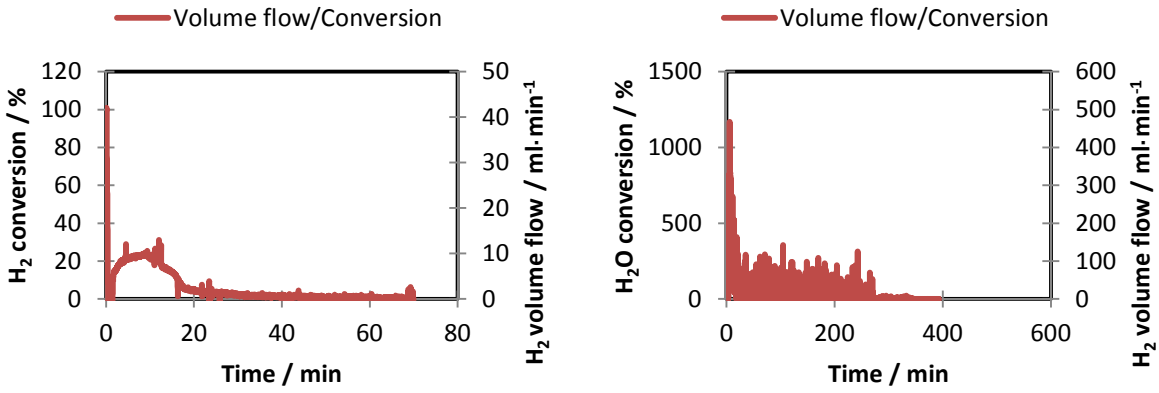


**Figure 29: Reduction (left) and oxidation (right) of the 1st cycle (5th series).**

Figure 29 – left displays the volume flow consumed by the reaction and indicates the fact that the contact mass contains at least some oxidized species.

The oxidation was performed with a high flow of steam of 0.36 g/min at automatically regulated pressure of 9 bar. The high flow leads to quick regulation time, though the conversion depicted is not significant for the reaction, as the flow is pulsating. It is visible in Figure 29 – right at about 350 minutes that there is no further reaction taking place – the volume flow has completely decreased. The oxidation can thus be considered finished at fully oxidized contact mass.

### 3.6.2 Second cycle

In this cycle the inherent problem of using unstabilised sponge iron is clearly observable. The reactivity as well as the overall applicability of this kind of contact mass seems to be limited because of sinter effects.

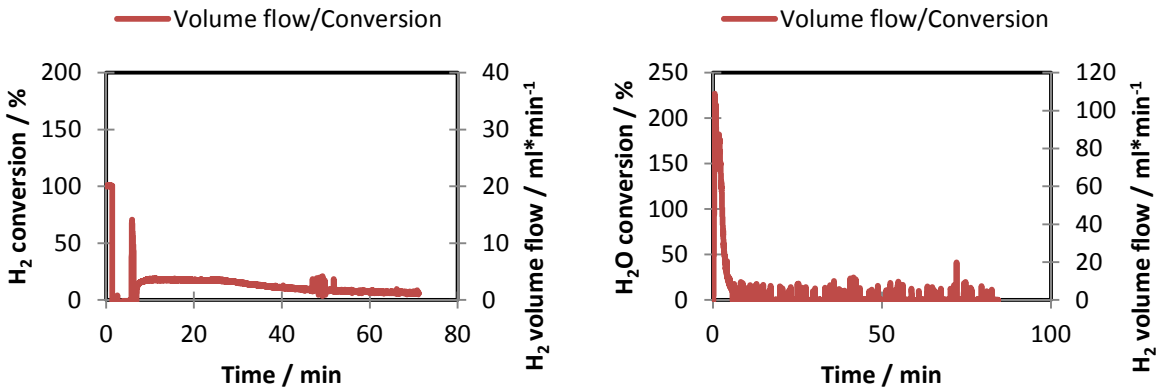


**Figure 30: Reduction of the 2nd cycle (5th series).**

During the reduction a high conversion at the beginning seems to indicate the presence of hematite $Fe_2O_3$, though thermodynamically only magnetite $Fe_3O_4$ would be possible. This phase of total $H_2$ conversion is followed by a period of no conversion at all (Figure 30 – left). These effects, combined with the resulting low yield give rise to the assumption that the reactor was blocked at the beginning. This prevents any gas reaching the analysis system and leads to a signal similar to total conversion. When the contact mass finally is partly reduced and the resulting pressurized hydrogen forced its way through, the excess of $H_2$ signifies too much hydrogen per minute. Finally, the pressure is in equilibrium with the ambient and the gas amounts are again correctly plotted, giving a reduction similar to the previous experiments.

The oxidation (Figure 30 – right) can be compared to the oxidation of the first cycle, although the time until the volume flow drops to zero is much shorter. The much shorter period of time until the end is directly related to the reactivity of the contact mass. Table 12 gives the impression of lost activity – not even 10 % of the hydrogen produced in the first cycle could be generated in this cycle.

### 3.6.3 Third cycle

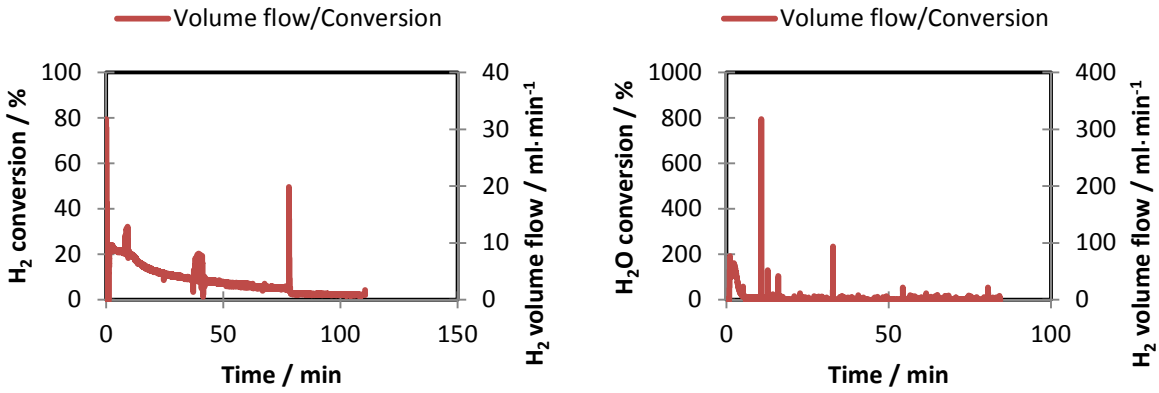


**Figure 31: Reduction (left) and oxidation (right) of the 3rd cycle (5th series).**

Also in the third series, a short period of very high apparent conversion is followed by no conversion at all. These effects are discussed above and lead to problems in evaluation. After about 75 minutes the $H_2$ stream was increased to about 70ml/min (Figure 31 – left).

The subsequent oxidation in its course still is similar to the previous cycles, though even less hydrogen is produced. A period of high conversion is followed by a long time of nearly no $H_2$ generation (Figure 31 – right).

Due to the nature of the pressure regulating system, also this experiment shows the characteristic pulsation in flow.

### 3.6.4 Results

The first cycle shows quasi total conversion of the contact mass during the oxidation step. Following cycles display rather rapid degradation and thus could not offer viable data on converted hydrogen.

**Figure 32: Sintered piece of contact mass. Reactivity immensely decreased by formation of such tight blocks.**

The entries for the third cycle show the phenomenon of more hydrogen consumption in the reduction than produced in the previous oxidation. This can be explained with the pressure build-up at the beginning because of sintering in the contact mass and subsequent breaking of these sintered pieces, offering slightly more active area than before. The oxidation though yields significantly lower amounts of hydrogen than before which indicates heavy losses in active surface due to sintering. The retrieval of the contact mass from the reactor proved to be hard because of the formation of one solid block. Gases seem to have passed mainly between the reactor wall and the contact mass, not through it (Figure 32).

**Table 12: Results of the 5$^{th}$ series.**

| Reaction | $H_2$ / mmol | $H_2$ / ml | $H_2$ conversion / % | $H_2O$ conversion / % | $H_2$ / mmol·g-1 | Contact mass conversion / % |
|---|---|---|---|---|---|---|
| Reduction 1 | 5.23 | 117.26 | 4.00 | - | 0.94 | 3.96 |
| Oxidation 1 | 129.00 | 2889.51 | - | 16.12 | 23.27 | 97.46 |
| Reduction 2 | 7.16 | 160.42 | 6.67 | - | 1.29 | 5.41 |
| Oxidation 2 | 10.19 | 228.27 | - | 6.05 | 1.84 | 7.70 |
| Reduction 3 | 14.34 | 321.32 | 7.38 | - | 2.59 | 10.84 |
| Oxidation 3 | 6.78 | 151.91 | - | 4.03 | 1.22 | 5.12 |

## 3.7 Sixth experimental series

The contact mass *Fe/Al$_2$O$_3$ 10%* was used in this series. Pressure control and maintenance was performed via a close mass flow controller at the exit of the system. This MFC could also be used as a mass flow meter to detect the amount of hydrogen during the experiments under the condition that no other gases are present in the product gas.

**Table 13: Contact mass of the 6$^{th}$ series.**

| Contact mass | Contact mass / g | reactive contact mass / mmol | max $H_2$ / mmol |
|---|---|---|---|
| Fe/$Al_2O_3$ 10 wt% | 6.09 | 98.14 | 130.85 |

### 3.7.1 First cycle

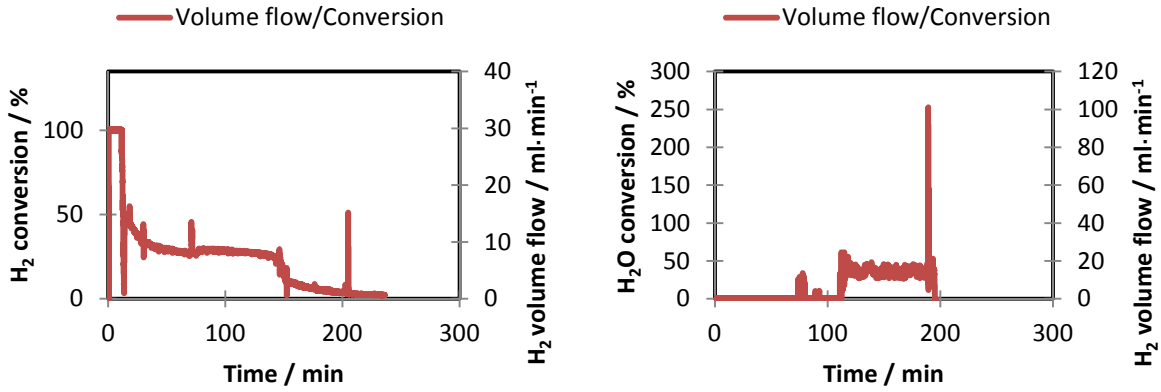


**Figure 33: Reduction (left) and oxidation (right) of the 1$^{st}$ cycle (6$^{th}$ series).**

The reduction was performed with a stream of 35 ml/min of hydrogen for most of the time. For the terminal phase the gas flow was doubled to 70 ml/min, visible in Figure 33 – left as the high peak resulting from switching the mass flow controller. Again, high initial conversion indicates the presence of the highly oxidized species of hematite created during sample calcinations in the electric oven under atmospheric conditions.

During the oxidation, 0.04 g/min of steam were used to produce hydrogen which consecutively built up 7.5 bar of pressure against the mass flow controller at the exit of the test rig at a constant product gas flow of 15 ml/min set in the MFC. The initial peaks at 75 and 90 minutes (Figure 33 – right) are related to leakage at the exit MFC due to insufficiently set operation parameters. After reaching the operating pressure, the gas flow was set. The experiment was terminated after the pressure and thus the conversion decreased to almost zero (Figure 33 – right, after 195 minutes).

Minor pulsation was still observable in this setup, though no regulation is needed. This pulsation of the product gas stream mass flow seems to be related only to the HPLC pump's pulsation.

### 3.7.2 Second cycle

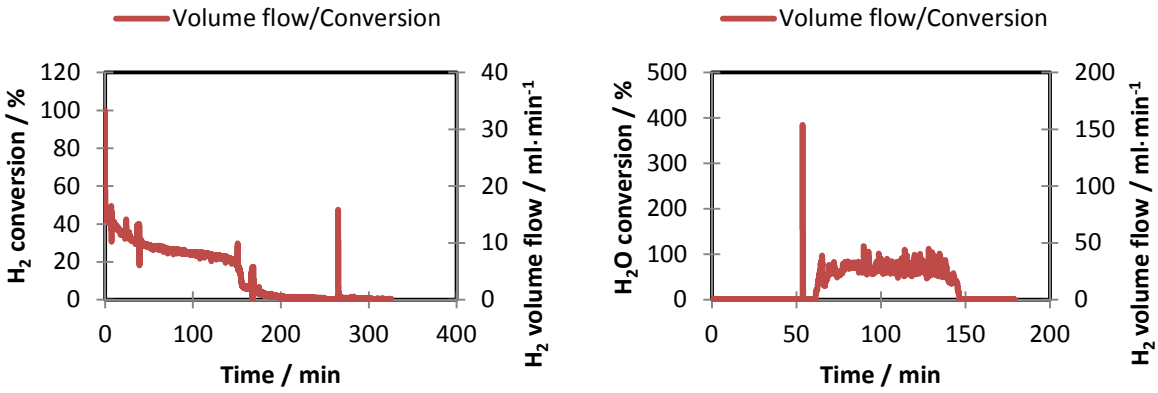


**Figure 34: Reduction (left) and oxidation (right) of the 2nd cycle (6th series).**

In this cycle a gas flow of 354 ml/min of $H_2$ was used to reduce the contact mass form its $Fe_3O_4$ state, so total conversion was not observable. The last high peak indicates the switching to higher flows – 70 ml/min of hydrogen were used at the end (Figure 34 - left).

An alternative water supply system had been installed. Water was delivered into the evaporator via an external tank under increased pressure of 7 bar of synthetic air. The flow was regulated by a Bronkhorst liquid flow controller. The oxidation was done by a 0.03 g/min flow of steam without increased pressure. The initial peak was related to switching from bypass to reactor.

### 3.7.3 Third cycle

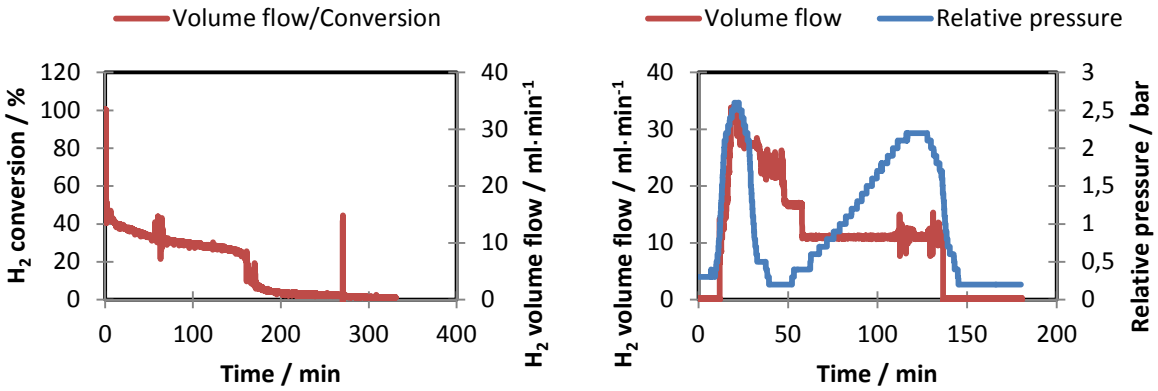


**Figure 35: Reduction (left) and oxidation (right) of the 3rd cycle (6th series).**

Reduction again was achieved by 35 ml/min of hydrogen gas at 750°C and atmospheric pressure. Again the experiment was completed by a stream of 70 ml/min of $H_2$.

As the oxidation was planned as a pressure experiment, the exit MFC was closed. A relative pressure of 2 to 3 bar was intended, but a constant flow with only 5 to 4 bar pressure difference between supply and reactor could not be maintained. Figure 35 – right showed the loss of internal pressure, as the flow of 35 ml/min was set and even at a decrease to

about 10 ml/min of product gas flow, the internal pressure could hardly be reached during the reaction time.

### 3.7.4 Results

More production than consumption of hydrogen during the first cycle occurred because of not fully oxidized contact mass after the calcinations. The difference in production and consumption in the second cycle is rather severe and could not be explained at this time. The cycle's reduction showed high consumption of $H_2$ relative to the previous oxidation; the oxidation, though operated in a previously untested way, yielded a comparable amount of hydrogen (Table 14).

**Table 14: Results of the 6th series.**

| Reaction | $H_2$ / mmol | $H_2$ / ml | $H_2$ conversion / % | $H_2O$ conversion / % | $H_2$ / mmol·g$^{-1}$ | Contact mass conversion / % |
|---|---|---|---|---|---|---|
| Reduction 1 | 43.66 | 977.88 | 23.96 | - | 7.17 | 33.36 |
| Oxidation 1 | 60.51 | 1355.51 | - | 36.07 | 9.94 | 46.25 |
| Reduction 2 | 36.18 | 810.41 | 32.72 | - | 5.94 | 27.65 |
| Oxidation 2 | 93.76 | 2100.14 | - | 65.38 | 15.40 | 71.65 |
| Reduction 3 | 92.49 | 2071.78 | 17.28 | - | 15.19 | 70.68 |
| Oxidation 3 | 86.76 | 1943.47 | - | 41.67 | 14.25 | 66.31 |

## 3.8 Seventh experimental series

5.38 g of the contact mass $Fe/Al_2O_3$ 20% were used in this series and held constantly under 750°C with no cool down phases between cycles or even experiments, as TGA experiments showed increased contact mass stability under this condition. The system was considered incapable of pressure build-up, as the pressure gradient form supply tank to reactor was too low.

**Table 15: Contact mass of the seventh series.**

| Contact mass | Contact mass / g | reactive contact mass / mmol | max $H_2$ / mmol |
|---|---|---|---|
| $Fe/Al_2O_3$ 20 wt% | 5.38 | 77.06 | 102.75 |

### 3.8.1 First cycle

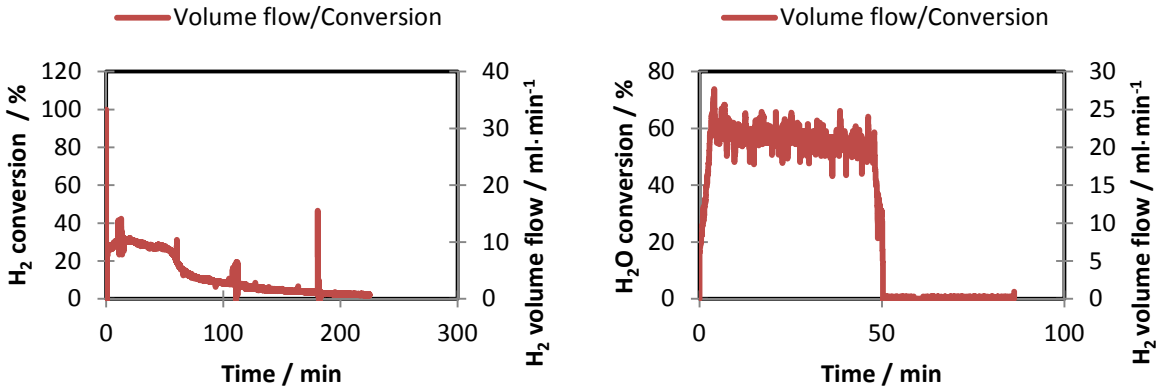


**Figure 36: Reduction (left) and oxidation (right) of the 1st cycle (7th series).**

Like in the previous reductions a flow of 35 ml/min of hydrogen was initially used, the experiment was finished by a period of 45 minutes at 70 ml/min.

The low conversion at the beginning indicates that there is almost no highly oxidized species present so the oxidation during sample preparation seemed to be of low extent.

The oxidation was carried out by 0.03 g/min of steam at ambient pressure. The exit mass flow controller was set to maximum to detect the product gas flow.

### 3.8.2 Second cycle

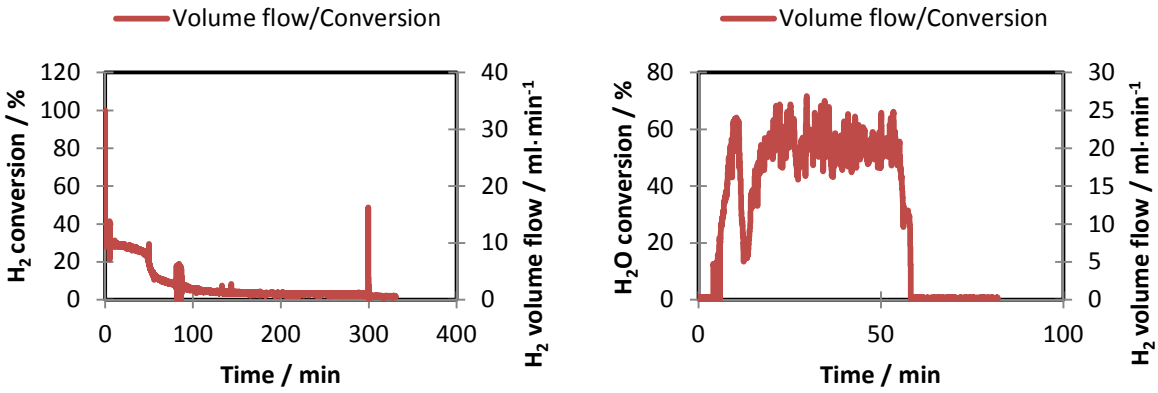


**Figure 37: Reduction (left) and oxidation (right) of the 2nd cycle (7th series).**

Also this cycle was performed with 35 ml/min and was finished with an increased stream of 70 ml/min, as visible by the peak near the end of the experiment (Figure 38 – left).

The oxidation again was done with 0.03 g/min of steam. The system was kept under ambient pressure; the exit mass flow controller was used as mass flow meter. A slight increase of pressure during the initial phase of the experiment prevented the supply of water, thus the volume flow and mean conversion dropped after about 15 minutes (Figure 37 – right). As the flow re-established, the experiment could be finished.

### 3.8.3 Third cycle

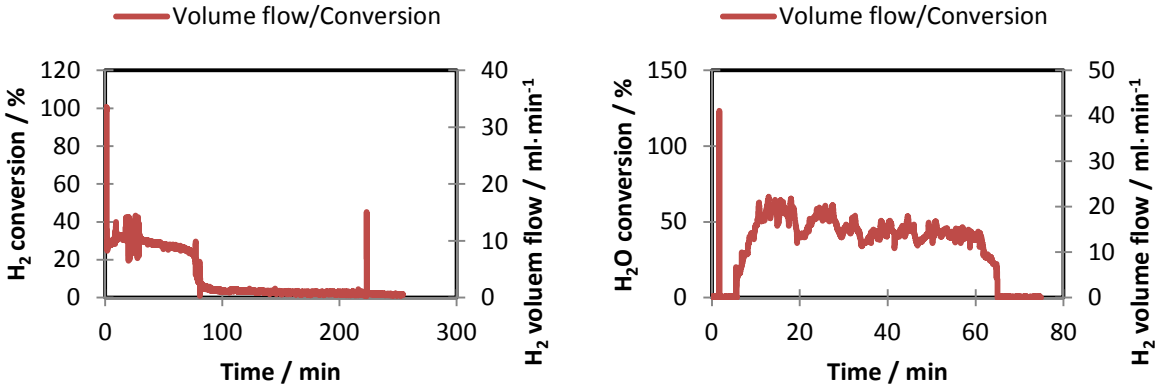


**Figure 38: Reduction (left) and oxidation (right) of the 3rd cycle (7th series).**

The reduction with 35 ml/min of $H_2$ was finished with 70 ml/min (Figure 38 – left). Like the first cycle's reduction this experiment showed an increase in conversion at the beginning. This could be related to an increase of reactive surface by the gas flow, which is slightly disrupting the fixed bed. The conversion rapidly dropped again because of the contact mass being reduced.

To perform the third oxidation a steam flow of 0.03 g/min was applied against ambient pressure (Figure 38 – right). The oxidation took slightly longer than the previous ones which is linked to the decrease of conversion. Approximately the same amount of hydrogen is produced, though over a longer period of time.

### 3.8.4 Results

Though a high conversion was achieved during the oxidation of the first cycle, the amount of hydrogen produced is significantly lower than in the previous series. The conversion and consumption of hydrogen during the reduction of the second cycle is comparable to the first cycle. The amount is still much lower than in other cycles with lower $Al_2O_3$ concentrations. Though the amount of aluminium oxide is slightly higher than in the previous cycles (20 % instead of 10 %), the converted amount of hydrogen significantly dropped about 50 %.

The higher consumption during the third reduction compared to the second oxidation's production could be related to the reason mentioned above - disturbance of the fixed bed and thus again increased reactivity.

**Table 16: Results of the 7th series.**

| Reaction | $H_2$ / mmol | $H_2$ / ml | $H_2$ conversion / % | $H_2O$ conversion / % | $H_2$ / mmol·$g^{-1}$ | Contact mass conversion / % |
|---|---|---|---|---|---|---|
| Reduction 1 | 41.93 | 1000.57 | 12.03 | - | 7.79 | 40.81 |
| Oxidation 1 | 45.36 | 1016.15 | - | 54.13 | 8.43 | 44.15 |
| Reduction 2 | 42.54 | 983.37 | 10.25 | - | 7.91 | 41.40 |
| Oxidation 2 | 44.21 | 990.20 | - | 49.64 | 8.22 | 43.02 |
| Reduction 3 | 46.02 | 1030.94 | 12.16 | - | 8.55 | 44.79 |
| Oxidation 3 | 43.80 | 981.01 | - | 44.23 | 8.14 | 42.62 |

## 3.9 Eighth experimental series

For the series 6.15 g of V7 contact mass (10 wt% of $Al_2O_3$ in $Fe_2O_3$) were used. The contact mass was kept at 750°C throughout the series, no cool-down phases were implemented over night.

**Table 17: Contact mass of the 8th series.**

| Contact mass | Contact mass / g | reactive contact mass / mmol | max $H_2$ / mmol |
|---|---|---|---|
| Fe/$Al_2O_3$ 10 wt% | 6.15 | 88.09 | 117.46 |

### 3.9.1 First cycle

The cycle was started with an oxidation by 100 ml/min of synthetic air for 30 minutes. This kind of pre-treatment was not recorded, as the contact mass should already be at its maximum oxidation state. It was done just to start at a defined condition.

The first reduction was performed at a flow of 35 ml/min of hydrogen. The experiment was sustained for 3.5 hours. After this period of time the cycle was considered finished. The data acquisition unfortunately failed, so no information about this cycle is present.

### 3.9.2 Second cycle

Also this cycle suffered from data record failure, so no information was acquired. The experiments were carried out as usual – oxidation with 0.03 g/min of steam; reduction with 35 ml/min of $H_2$.

### 3.9.3 Third cycle

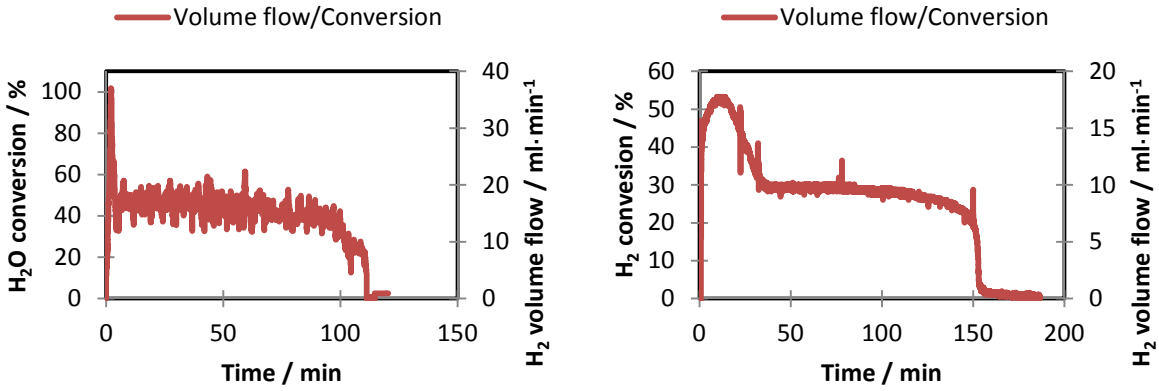


**Figure 39: Oxidation (left) and reduction (right) of the 3rd cycle (8th series).**

The cycle was started with an oxidation of the previously reduced contact mass with 0.03 g/min of steam at ambient pressure (Figure 39 – left). The initial peak of 85 % conversion could be related to some $H_2$ still present after the finished reduction of the second cycle. The

oxidation shows nearly constant reactivity for about two thirds of the reaction time, the decrease of reactivity is very steep, which indicates the end of the experiment.

The following reduction was achieved by means of a 35 ml/min flow of hydrogen. The experiment was carried out until the conversion of $H_2$ dropped to a value lower than 1 %. An initial increase in conversion again could be explained by the prior discussed surface enhancement due to the presence of a gas flow (see 3rd oxidation of the 7th series). The transition from FeO to Fe is observable quite well, though the earlier transition from higher oxidation states to wuestite FeO is not as clear, as there is no period of constant conversion of the higher oxidation states.

### 3.9.4 Fourth cycle

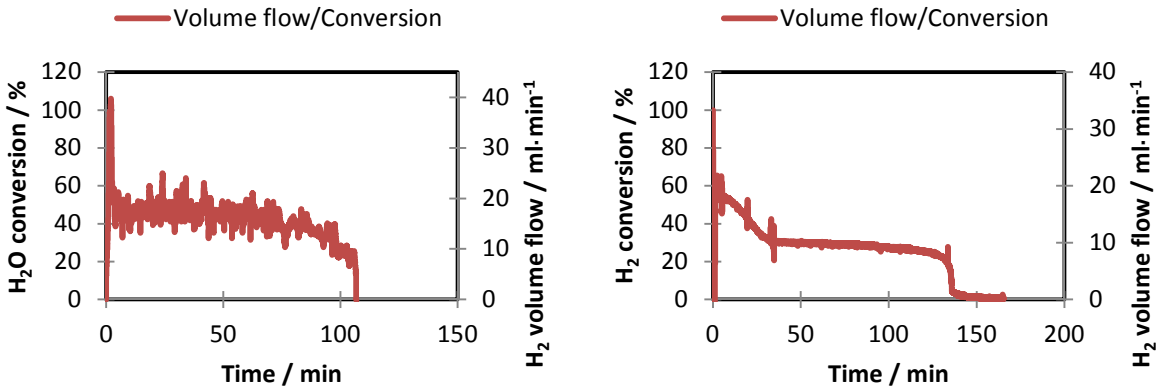


**Figure 40: Oxidation (left) and reduction (right) of the 4th cycle (8th series) – steam.**

In the fourth oxidation, a flow of 0.03 g/min of steam was used to reach the oxidation state of magnetite $Fe_3O_4$. This oxidation state represents the maximum thermodynamically achievable by steam. To reach the higher oxidation state of hematite $Fe_2O_3$, 50 ml/min of synthetic air were used.

The steam oxidation is quite comparable to the previous experiment. As air is a gas mixture, the micro GC was used to analyse the product gas stream during the second part of the oxidation. The maximum rate of measurement is one sample every 3 minutes. This proved to provide a resolution too low to identify the transitions of oxidation states or to quantify the amount of converted oxygen. After roughly 10 minutes the gas concentrations in the product gas stream were equal to the bypass concentrations – the contact mass was fully oxidized as no oxygen was consumed anymore.

Reduction of the fully oxidized species was done by a stream of 35 ml/min of $H_2$. Although the presence of highly oxidized contact mass provided reason to expect very high conversion of about 100 % at the beginning, much lower conversions of about 70 % did occur. These rapidly dropped to the familiar 30 % of the wuestite phase.

### 3.9.5 Fifth cycle

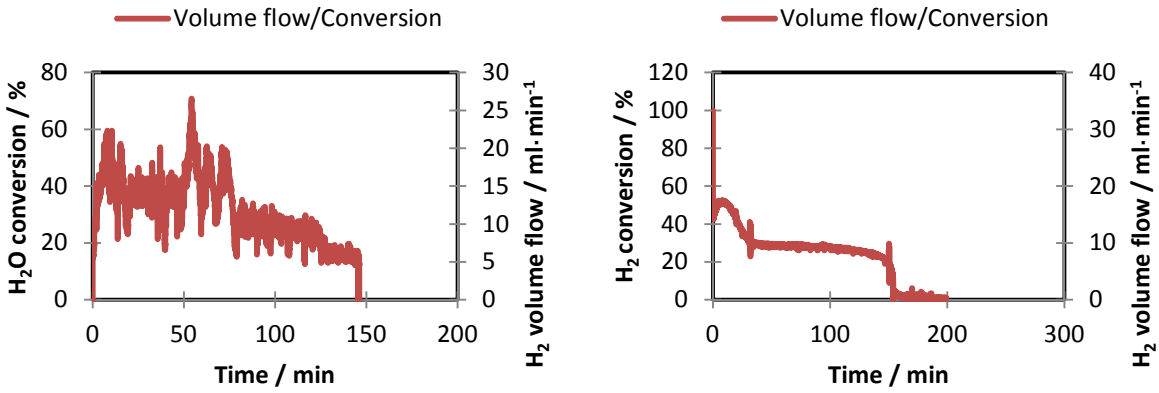


**Figure 41: Oxidation (left) and reduction (right) of the 5th cycle (8th cycle).**

Like the previous cycles, the streams were 0.03 g/min of steam for the oxidation. The reduction was done with 35 ml/min of hydrogen. Minor inconsistency in the oxidant's flow lead to the high conversion and product gas flow after about 50 minutes, the total amount should not be influenced by these effects.

During the reduction no period of high flow was started after reaching the lowest conversion step (after about 160 minutes). The experiment was finished after the conversion had dropped well below 1 %.

### 3.9.6 Sixth cycle

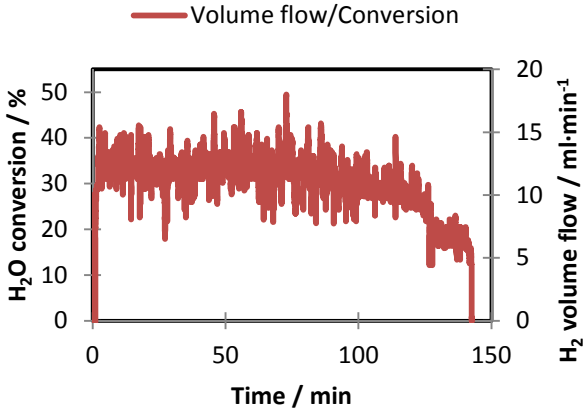


**Figure 42: Oxidation of the 6th cycle (8th series).**

The cycle in fact consists only of an oxidation performed with a steam flow of 0.03 g/min. To generate a pressure gradient from tank to evaporator, helium was used in these experiments.
In Figure 42 there are possibly two steps of different conversions present. This difference in conversions is directly related to different oxidation states of the contact mass. Due to the rather low signal-to-noise ratio, the effect was not that clearly observable though.

### 3.9.7 Results

Unfortunately no data could be obtained during the first and second cycle. The amount of hydrogen consumed during the reduction of the third cycle fits to the amount produced in the previous oxidation. Though the percentage of aluminium oxide in the contact mass is only slightly lower than in the previous series – 10 % compared to 20 %, the amount of converted and produced hydrogen per gram of contact mass is 33 % higher. This indicates a maximum in sensible additive concentration.

The reduction of the third cycle performed in a way expected. Slightly decreased $H_2$ uptake was observable.

Table 18 shows only the data of the steam oxidation of the fourth cycle – these are comparable to the previous cycle. The data obtained in the following reduction indicate degradation, as the reduction took up significantly lower amounts of hydrogen (10.84 mmol/g), although it started at a higher oxidation state.

In the fifth cycle the increased amount of produced hydrogen compared to the reduction of the fourth cycle (10.84 mmol/g) can be explained again by the slightly higher pressure in the reactor. These pressure pulses could have slightly disturbed the fixed bed and thus activated shut off areas of the bed. The supply tank with liquid flow controller proved to be prone to flow inconsistency.

The results are comparable to the other cycles and degradation has taken place to a minimal extent only.

**Table 18: Results of the 8$^{th}$ series; oxidation experiments followed by oxidations with air are marked with an *a*.**

| Reaction | $H_2$ / mmol | $H_2$ / ml | $H_2$ conversion / % | $H_2O$ conversion / % | $H_2$ / mmol·g$^{-1}$ | Contact mass conversion / % |
|---|---|---|---|---|---|---|
| Oxidation 3 | 78.30 | 1753.93 | - | 42.16 | 12.73 | 59.26 |
| Reduction 3 | 74.02 | 1658.13 | 26.60 | - | 12.04 | 56.02 |
| Oxidation 4 - *a* | 75.67 | 1695.08 | - | 42.56 | 12.30 | 57.27 |
| Reduction 4 | 66.70 | 1493.98 | 25.55 | - | 10.84 | 50.47 |
| Oxidation 5 | 76.04 | 1703.35 | - | 31.19 | 12.36 | 57.55 |
| Reduction 5 | 74.90 | 1677.82 | 23.22 | - | 12.18 | 56.68 |
| Oxidation 6 | 73.07 | 1636.80 | - | 30.73 | 11.88 | 55.30 |

## 3.10 Ninth experimental series

6.30 g of contact mass V7 (10 wt% of $Al_2O_3$ on $Fe_2O_3$) were used in this series (Table 19).

**Table 19: Contact mass of the 9th series.**

| Contact mass | Contact mass / g | reactive contact mass / mmol | max $H_2$ / mmol |
|---|---|---|---|
| $Fe_2O_3/Al_2O_3$ 10 wt% | 6.30 | 71.01 | 94.68 |

The series was initiated by an oxidizing step with 100 ml/min of synthetic air at 750°C for 30 minutes. This is considered as cycle zero for reasons of documentation. During the subsequent cycles, experiments under ambient pressure and increased pressure were performed. To minimize mechanical stress by thermal expansion and contraction, the temperature was kept at 750°C for the first three cycles and, after the weekend, for another four cycles.

The amounts of produced hydrogen deviate from the amounts of consumed $H_2$ due to problems with the peltier condenser's valve. During the pressure experiments the liquid-gas separator released also some of the product gas (Figure 43), which was not analysed and thus is missing in the results. Although the malfunctions of the valve system certainly also occurred during the experiments at ambient pressure, only at higher pressure the amount of $H_2$ forced through the lower tube was significant. This amount of "lost" gas could not be evaluated, as the problem was identified not before the end of the series.

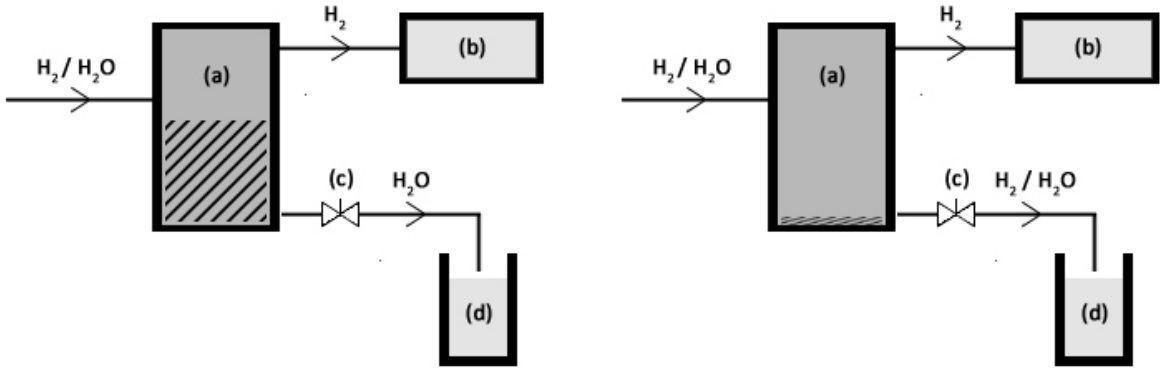


**Figure 43: Schematic view of the product gas mixture flow. Left – no gas leakage through the condenser (a) occurs due to filling level above the valve (c). Product gas stream takes the way to the analyser (b), condensed water is collected. Right – malfunction of the regulating valve system (c) leads to low filling levels. $H_2/H_2O$ mixture can pass through the lower tube.**

### 3.10.1 First cycle

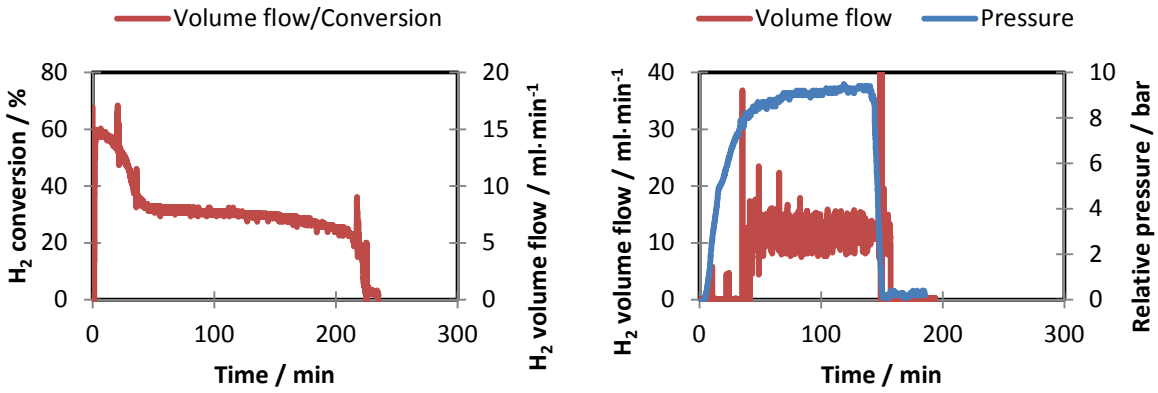


**Figure 44: Reduction (left) and oxidation (right) of the 1st cycle (9th series).**

The cycle started with a reduction at 750°C with a flow of 25 ml/min of hydrogen. The reduction, though performed after an oxidizing pre-treatment with synthetic air, did not show the characteristic high conversion of about 100 % when the hematite phase was reduced. The conversion of about 60 % corresponds to the magnetite-to-wuestite conversion.

The consecutive oxidation was achieved by a steam flow of 0.03 g/min at pressure greater than 8 bar. This operating pressure was reached after about 35 minutes (Figure 44). The pressure build-up was investigated more closely and is described later under *High pressure hydrogen*.

The initial peaks before the operation pressure was reached occurred because of minor leakage of the exit mass flow controller. The product gas volume flow was set to 10 ml/min to maintain high pressure without an excessive pressure increase. By design of the experimental setup pressure only derived from produced hydrogen.

### 3.10.2 Second cycle

Due to an incident at the recording system, no data had been acquired during the reduction. As the experiment's performance is independent of this system, the reduction was finished normally.

During the reduction a gas flow of 25 ml/min of $H_2$ was used at 750°C. There is no additional data available on this experiment.

The oxidation with 0.03 g/min of $H_2O_{(g)}$ was carried out under pressure greater than 8 bar at 750°C. The pressure build-up is also described under *High pressure hydrogen*.

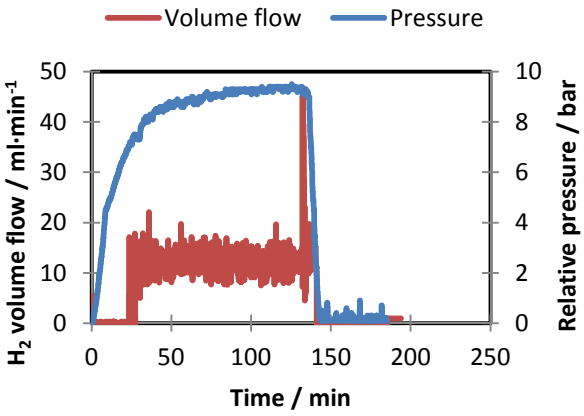


**Figure 45: Oxidation of the 2nd cycle (9th series).**

After reaching the operating pressure, the product gas flow was set to 10 ml/min of hydrogen to be released. Similar to the previous oxidation (Figure 44 – right), Figure 45 shows that the end of the reaction was reached at a defined moment. There is no such thing as a declining reactivity at the present gas flows.

## 3.10.3 Third cycle

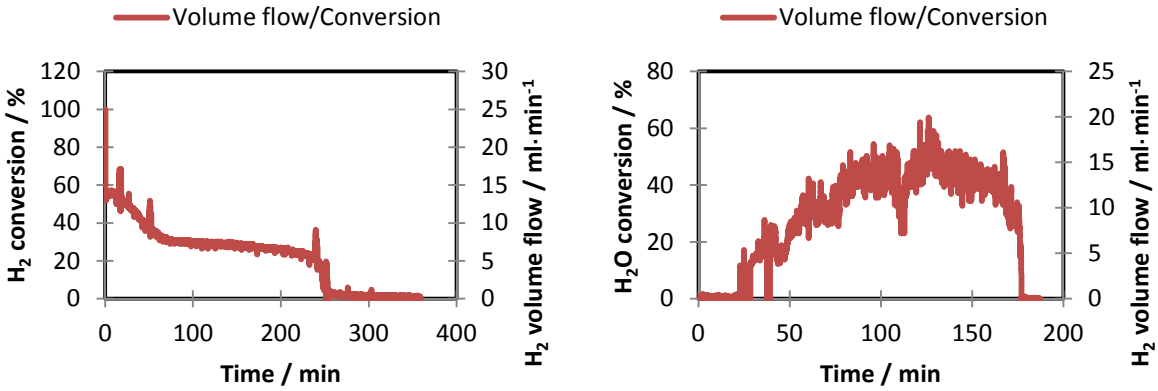


**Figure 46: Reduction (left) and oxidation (right) of the 3rd cycle (9th series).**

Reduction of the contact mass was achieved by 25 ml/min of hydrogen at 750°C. The reduction took about 25 minutes longer than the reduction of the second cycle (Figure 44) because of higher hydrogen consumption (Table 21). Some kind of conditioning of the contact mass could be postulated at this point.

The oxidation of the 3rd cycle was a two-part experiment. The first part consisted of an oxidation with 0.03 g/min of steam, the second part consisted of oxidizing to a higher oxidation state by a stream of 100 ml/min of synthetic air. Both parts were carried out at 750°C and at ambient pressure.

The steam oxidation (Figure 46) showed an increase in conversion for about 100 minutes, followed by a decrease for about 50 minutes. The end of the experiment is visible by a very steep decrease to conversion lower than 1 %.

The increase (from 25 to 125 minutes) and decrease (till the end) can be explained by back-mixing and thus dilution of the product gas with steam as it travels over the contact mass bed. During the progressive oxidation, the product gas is generated in a zone shifted towards the exit end of the reactor – reactions occur mainly in this zone and the thermodynamic equilibrium is achieved. As the produced hydrogen backmixes with steam, the amount of hydrogen per time unit at the exit is much lower than the amount really produced. At the end of the reaction, the diluted product gas reaches the analysis system. The amount of produced gas decreases, as reactive material in low oxidation states is no longer available. Once the whole contact mass bed is oxidized and the backmixed gas reached the exit MFC, the oxidation's conversion dropped to <1 %.

The oxidation by 100 ml/min of synthetic air took only few minutes. Time resolution is limited, as the gas chromatograph analysed one sample every 3 minutes. Once the oxygen concentration in the product gas reached the initial concentration of 20.5 %, the experiment was considered finished. The exact amount of taken up oxygen is not quantifiable.

### 3.10.4 Fourth cycle

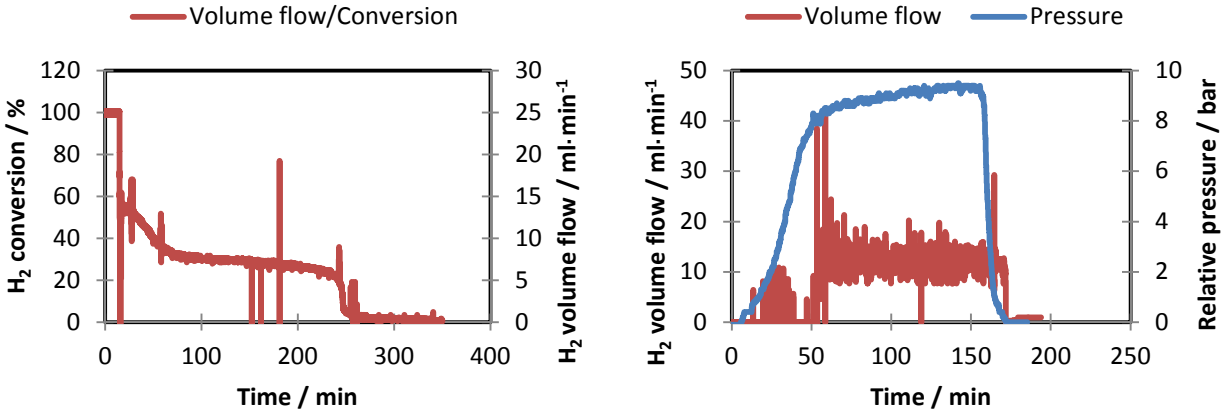


**Figure 47: Reduction (left) and oxidation (right) of the 4th cycle (9th series).**

The fourth cycle's reduction was carried out with a stream of 25 ml/min of hydrogen. The high oxidation state of the contact mass was previously achieved by oxidizing with synthetic air (3rd cycle).

Initially, there is was a period of high conversion corresponding to the hematite proportion in the fixed bed. There could have been some air present in the product gas tubing which reached the exit mass flow controller only after it was pushed into MFC by some of the non-converted hydrogen. The mass flow controller then massively over-detected the "wrong" gas and thus gave a high signal corresponding to zero conversion. The low conversion at about 150 minutes and the peak at 180 minutes are related to only one measurement (1.2 seconds) and is maybe related to minor flow discrepancy.

Also during this oxidation some gas leaked through the closed analyser MFC. This was subsequently prevented by setting the mass flow controller to -10 ml/min. The flow was maintained by the HPLC pump delivering 0.03 g/min of steam, when 10 ml/min were let out. As long as the conversion was high enough, the pressure was held up.

### 3.10.5 Fifth cycle

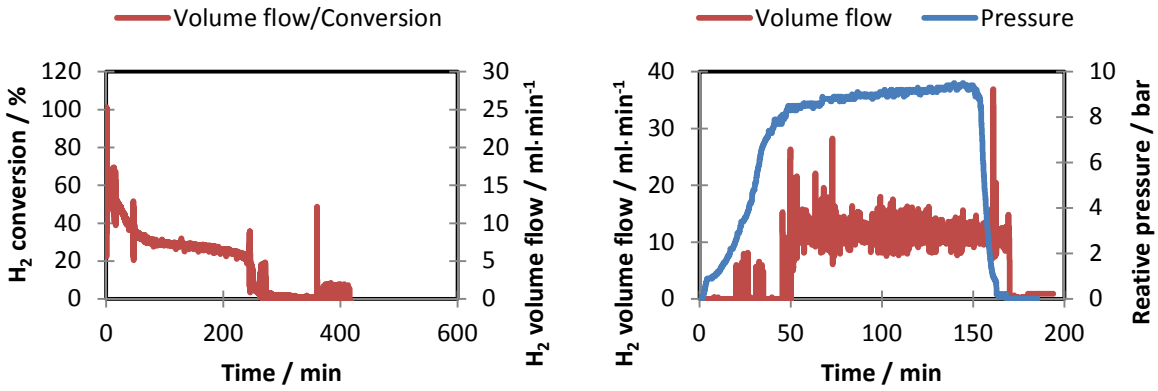


**Figure 48: Reduction (left) and oxidation (right) of the 5th cycle (9th series).**

The reduction of this cycle was performed with a stream of 25 ml/min of hydrogen for 360 minutes (Figure 48 – left). Then the stream was doubled to achieve maximum conversion of the contact mass in a short period of time.

For the oxidation 0.03 g/min of steam were used. The pressure build-up is described later. To generate a continuous flow of product hydrogen, the exit MFC was opened slightly to 10 ml/min. As visible in Figure 48 – right, the pressure still increased after that point and the flow of $H_2$ was initiated. Like in the previous cycle, pressure and hydrogen flow decreased to zero after the conversion of the contact mass was done.

### 3.10.6 Sixth cycle

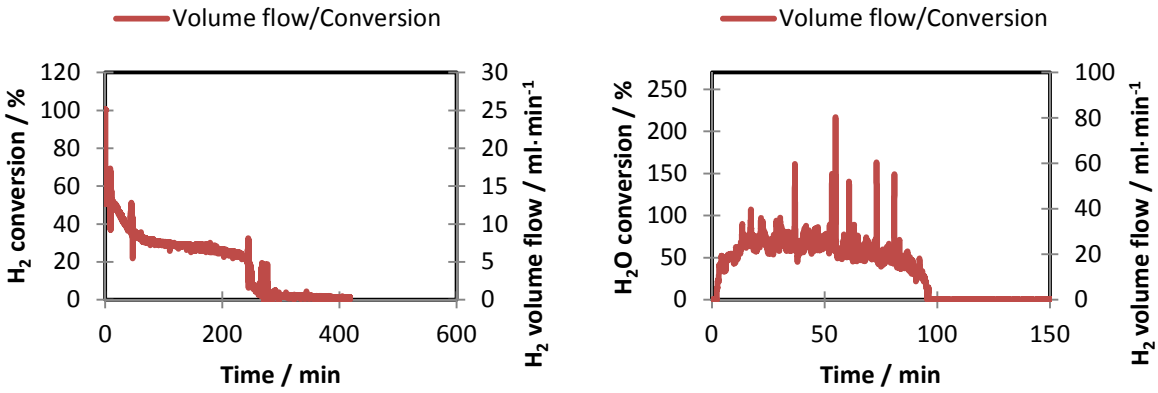


**Figure 49: Reduction (left) and oxidation (right) of the 6th cycle (9th series).**

During this cycle's reduction, the flow of 25 ml/min of hydrogen was not doubled at the end. Experimental time appeared to be long enough to achieve full contact mass conversion.

The oxidation was performed in two stages. At first, an oxidation is performed with 0.03 g/min of steam at ambient pressure. After the steam oxidation, a stream of 50 ml/min of synthetic air was used to fully oxidize the contact mass. Analysis of the oxidation with air was done by micro GC. As the gas chromatograph could acquire data only every three minutes and the oxidation took only about 15 minutes, time resolution was very low.

### 3.10.7 Seventh cycle

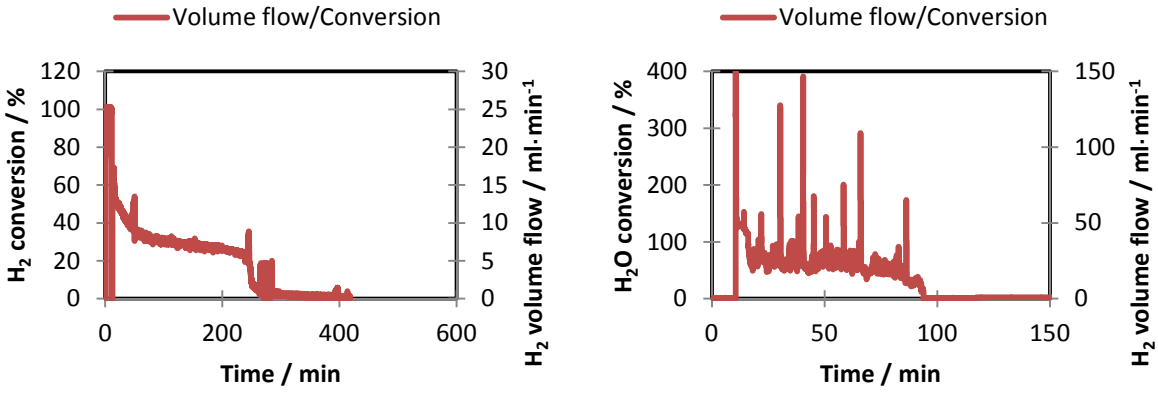


**Figure 50: Reduction (left) and oxidation (right) of the 7th cycle (9th series).**

This cycle (Figure 50) was done in the same way as the previous one. Reduction with 25 ml/min of $H_2$, oxidation with 0.03 g/min of $H_2O_{(g)}$ followed by 50 ml/min of synthetic air for 15 min. The cycle was carried out at 750°C and ambient pressure.

### 3.10.8 Eighth cycle

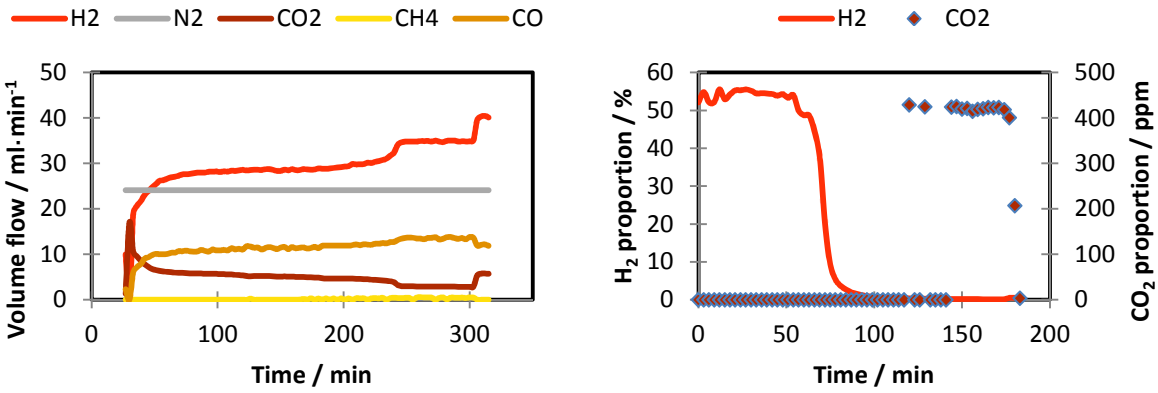


**Figure 51: Reduction with syn-gas mixture (left) and oxidation (right) of the 8th cycle (9th series).**

The reduction was performed at 750°C with an artificial syn-gas mixture consisting of hydrogen, carbon monoxide and carbon dioxide. Nitrogen had to be added as internal standard for quantification of the reactive gases. The composition of the gas mixture is visible in Table 20. After evaluating the gas flows in bypass operation, the reaction was started. After a rapid decline of reducing gas conversion – the flow leaving the reactor increased (Figure 51 – left, minutes 30 to 60) – a plateau was reached. After further reducing the contact mass, a second decrease of gas conversion at about 245 minutes appeared. This second plateau did not correspond to the gas composition measured in bypass, so reactions did still take place. As $CO_2$ concentration at the analyser did further decrease it was obvious, that $CO_2$ is used up in these reactions. Several side reactions were proposed at this point (see Results). After a total of 300 minutes, the system was switched to bypass to compare the gas flows again.

**Table 20: Syn-gas mixture composition (evaluated by bypass).**

| Gas | Flow / ml·min$^{-1}$ | Proportion / % |
|---|---|---|
| $H_2$ | 40.0 | 49.9 |
| CO | 10.5 | 13.1 |
| $CO_2$ | 5.6 | 7.0 |
| $N_2$ | 24.1 | 30.0 |

The oxidation of this cycle was done by 0.03 g/min of steam in 25 ml/min of nitrogen at pressure greater than 8 bar. Nitrogen again acted as internal standard for the analysis. The GC had to be used to eventually detect carbonaceous contaminants, which deposited during reduction and could be set free by oxidation. Only after total conversion of the contact mass – hydrogen generation is finished – $CO_2$ is produced from the carbon deposits on the contact mass (Figure 51 – right).

### 3.10.9 Results

Table 21 displays the collected results of the 9$^{th}$ series with exception of the last cycle. This syn-gas cycle proved to be too complex to fit into the table; its results are described separately.

The difference in hydrogen consumed and produced in the first cycle is about 18 %. 11 % difference is related to the highest achievable oxidation state of magnetite, as the higher oxidation state of hematite is not reachable and thus less hydrogen is produced. The peltier condenser's malfunction could have led to the rest in difference. In the second cycle, no data about the reduction could be acquired. The oxidation though is comparable to the previous oxidation. This gives rise to the assumption that the 17 % difference to the reduction of the second cycle could mainly be related to the peltier condenser problems. Because pressure was not increased during the oxidation at the 3$^{rd}$ cycle, the liquid-gas separator did not let out product gas. In fact the produced amount of hydrogen fits tightly to the amount consumed during the reduction.

In the 4$^{th}$ cycle, the hydrogen consumption of the reduction was significantly higher than during the previous cycle because of the higher oxidation state of the contact mass. The higher oxidation state had been achieved by oxidation by synthetic air, thus the contact mass conversion had to be calculated with the oxidation number of $Fe^{III}$ in hematite. The excess of hydrogen conversion compared to the previous oxidation is about 8 %. The presence of $Fe_2O_3$ should allow up to 11 % more converted hydrogen compared to $Fe_3O_4$, though degradation of the contact mass could have led to the lower value.

The 5$^{th}$ cycle's reduction was quite comparable to the reduction of the 3$^{rd}$ cycle. The oxidation's hydrogen yield was lower because of condenser leakage. During the 6$^{th}$ cycle, high amounts of hydrogen could be converted and generated respectively. The reduction fits to previous cycles; the oxidation was performed against ambient pressure, so no significant leakage occurred. Finishing the oxidation with synthetic air led to the high conversion of the following cycle.

A high amount of converted hydrogen in the 7$^{th}$ cycle's reduction corresponds to the highly oxidized species of hematite achieved in the 6$^{th}$ cycle. The contact mass conversion had to be related to the oxidation number of $Fe^{III}$. Performing an oxidation against ambient pressure did not lead to leakage. Thus a high amount of hydrogen could be detected.

**Table 21: Results of the 9th series; oxidation experiments followed by oxidations with air are marked with an *a*; a $^{h}$ indicates the presence of hematite during this reaction.**

| Reaction | $H_2$ / mmol | $H_2$ / ml | $H_2$ conversion / % | $H_2O$ conversion / % | $H_2$ / mmol·g$^{-1}$ | Contact mass conversion / % |
|---|---|---|---|---|---|---|
| Reduction 1 | 75.00 | 1679.96 | 29.79 | - | 11.90 | 79.21 |
| Oxidation 1 | 61.69 | 1381.87 | - | 26.21 | 9.79 | 65.15 |
| Reduction 2 | * | * | * | - | * | * |
| Oxidation 2 | 60.52 | 1355.68 | - | 26.33 | 9.61 | 63.92 |
| Reduction 3 | 88.28 | 1977.43 | 32.62 | - | 14.01 | 93.24 |
| Oxidation 3 - *a* | 90.11 | 2018.49 | - | 36.30 | 14.30 | 95.17 |
| Reduction 4 | 97.73 | 2189.07 | 33.96 | - | 15.51 | 91.75$^{h}$ |
| Oxidation 4 | 62.39 | 1397.51 | - | 20.88 | 9.90 | 65.89 |
| Reduction 5 | 88.75 | 1987.94 | 30.52 | - | 14.09 | 93.73 |
| Oxidation 5 | 61.71 | 1382.31 | - | 24.72 | 9.80 | 65.18 |
| Reduction 6 | 91.45 | 2048.51 | 30.56 | - | 14.52 | 96.59 |
| Oxidation 6 - *a* | 91.22 | 2043.40 | - | 58.69 | 14.48 | 96.35 |
| Reduction 7 | 98.20 | 2199.72 | 32.62 | - | 15.59 | 92.19$^{h}$ |
| Oxidation 7 - *a* | 91.84 | 2057.21 | - | 59.04 | 14.58 | 97.00 |

The 8th cycle's reduction was performed until after a total of 300 minutes an equilibrium state was reached. At this time, no changes in gas flows were observable – continuous reactions between the gases could be proposed. Hydrogen as well as carbon dioxide was still used up in the reactor. These seem to be the educts. More carbon monoxide left the reactor than the bypass. Methane left the reactor, but not the bypass. CO and $CH_4$ are products of the reactions. Comparison between the bypass operation's gas flows and the reactor gas flows offers the data for the following considerations.

Considering the apparent amounts of gas converted and produced during the syngas cycle's reduction, the acquired data does not match reality. Hydrogen conversion could be sustained up to any time and the continuous reaction will always run and convert. By calculating the relevant stoichiometric coefficients for the side reactions (Equation 28, Equation 29 and Equation 30), the apparent $H_2$ and $CO_2$ over-consumption as well as the CO overproduction (Table 22) can be all but compensated. This gives the corrected result data for the reduction of the 8th cycle.

$$CO_2 + H_2 \rightarrow CO + H_2O \qquad \Delta H_{298} = +41.2 \text{ kJ/mol} \qquad (28)$$

$$CO + 3\,H_2 \rightarrow CH_4 + H_2O \qquad \Delta H_{298} = +241.8 \text{ kJ/mol} \qquad (29)$$

$$CO + H_2 \rightarrow C + H_2O \qquad \Delta H_{298} = -153.7 \text{kJ/mol} \qquad (30)$$

**Table 22: Reactive gases for syn-gas side reactions, educts marked with *.**

| Gas | Volume / ml | Amount / mmol |
|---|---|---|
| $H_2$* | 392.7 | 15.5 |
| CO | 105.8 | 9.2 |
| $CO_2$* | 205.7 | 1.9 |
| $CH_4$ | 43.6 | 4.7 |

Oxidation of the contact mass yielded very pure hydrogen for most of the experimental time. At the end though, after the hydrogen formation was finished (by reason of fully oxidized iron contact mass), $CO_2$ was detected. By oxidizing the carbon previously deposited during reduction these contaminant species were released (Equation 19). The amount of $CO_2$ emitted is less than 450 ppm and refers to hydrogen purity of >99.9%.

Another possible explanation would be the dilution of the $CO_2$. Emission of $CO_2$ throughout the whole oxidation could have occurred, but only when the $H_2$ stream did decrease, the $CO_2$ concentration was high enough to be detected.

Comparison between the reduction and the oxidation of the 8$^{th}$ cycle shows the discrepancy of about 10 %. This can be explained by progressive degradation of the contact mass as well as by the possibility of further side reactions occurring and not taken into account during the calculation.

**Table 23: Results of the 8$^{th}$ cycle (9$^{th}$ series), showing the apparent and the side reaction corrected amounts of substance; a $^{h}$ indicates the presence of hematite during this reaction. A * during the reduction indicates the total amounts of reductant – $H_2$ and CO are consumed.**

| Reaction | $H_2$ / mmol | $H_2$ / ml | $H_2$ / mmol corr | $H_2$ / ml corr | $H_2$ / mmol·g$^{-1}$ | Contact mass conversion / % |
|---|---|---|---|---|---|---|
| Reduction 8 | 119.22* | 2670.54* | 101.69* | 2277.81* | 16.14* | 95.46$^{h}$ |
| Oxidation 8 | 91.67 | 2053.39 | - | - | 14.55 | 96.82 |

This series is characterized by very high conversions of contact mass. This could possibly refer to the quality of sample preparation, as this series' contact mass was mechanically mixed powder instead of wet impregnated iron.

## 3.11 Tenth experimental series

In this series 6.06 g of contact mass V2 (10 wt% of $Al_2O_3$ on $Fe_2O_3$) were used.

**Table 24: Contact mass of the 9th series.**

| Contact mass | Contact mass / g | reactive contact mass / mmol | max $H_2$ / mmol |
|---|---|---|---|
| $Fe_2O_3/Al_2O_3$ 10 wt% | 6.06 | 68.31 | 91.08 |

At this point another way of analysis was implemented. The product gas stream was led into one of the non-used on-board mass flow controllers of MICROACTIVITY-Reference, which in turn was operated similarly to the previous setup – closed for pressure build-up and slightly open for a controlled stream of hydrogen. By this setup, the comparability should be increased by using MFCs of the same type.

The experimental series was started with a reduction experiment. All experiments were carried out at 750°C. To minimize stress to the contact mass, the temperature was held at this level for the first, second and third cycle. For the 4th cycle the system was again checked to be gas tight, the heating was switched off for maintenance.

### 3.11.1 First cycle

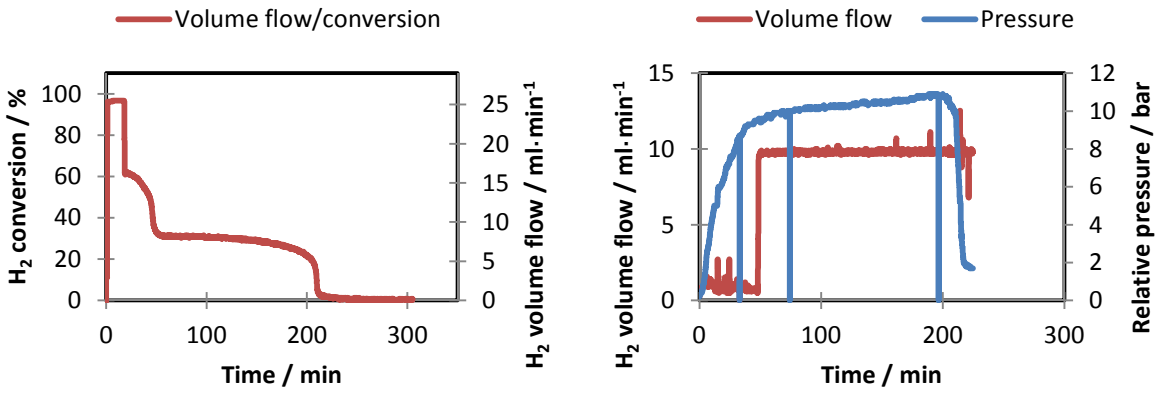


**Figure 52: Reduction (left) and oxidation (right) of the 1st cycle (10th series).**

This cycle started with a reduction at 750°C with a flow of 25 ml/min of hydrogen. Again initially high conversion of hydrogen and clear transitions through the various states of oxidation were observable (Figure 52 – left).

During the oxidation at raised pressure, performed with a stream of 0.03 g/min of steam the liquid-gas separator had to be operated manually. The three pressure drops during the experiment were related to these operations. The sudden stop of the experiment after about 225 minutes was related to malfunction of the exit mass flow controller due to moisture passing the peltier element.

### 3.11.2 Second cycle

The second cycle's reduction was performed with 25 ml/min of H2 at 750°C. Evaluating the stream before the experiment by measuring the bypass flow was done for five minutes.

The consecutive oxidation was done at ambient pressure at 750°C with a steam flow of 0.03 g/min (Figure 53 – right).

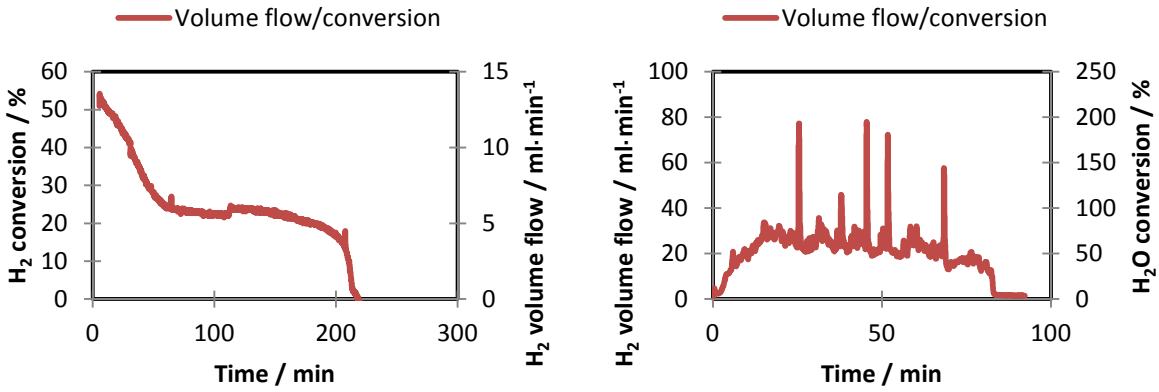


**Figure 53: Reduction (left) and oxidation (right) of the 2nd cycle (10th series).**

### 3.11.3 Third cycle

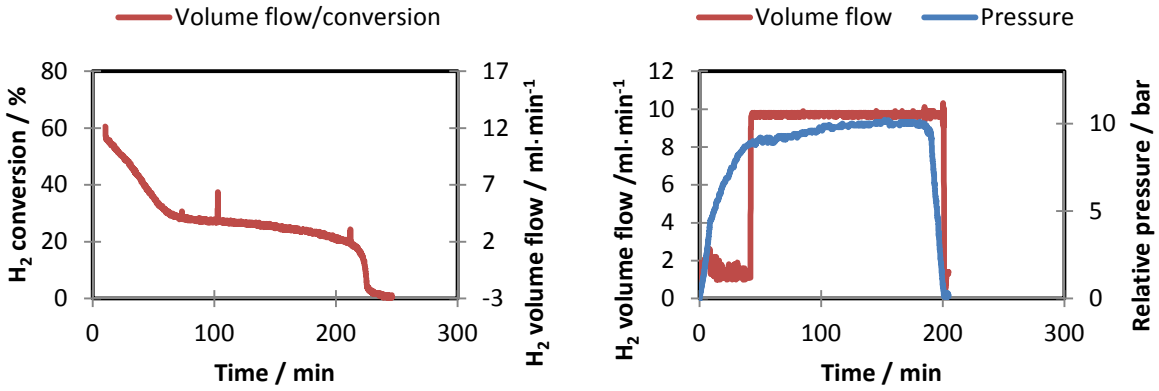


**Figure 54: Reduction (left) and oxidation (right) of the 3rd cycle (10th series).**

Again the reduction was carried out at 750°C wit 25 ml/min of hydrogen. The oxidation was performed at increased pressure of 8 to 10 bar with a flow of 0.03 g/min of steam.

Transitions of the various oxidation states were observable during the reduction. During the oxidation the correlation of pressure build-up and hydrogen generation is once again clearly visible. Once there was no $H_2$ production anymore, the pressure decreased to ambient level. Pressure build-up during the phase of no present gas flow is covered in *High-Pressure Hydrogen.*

### 3.11.4 Fourth cycle

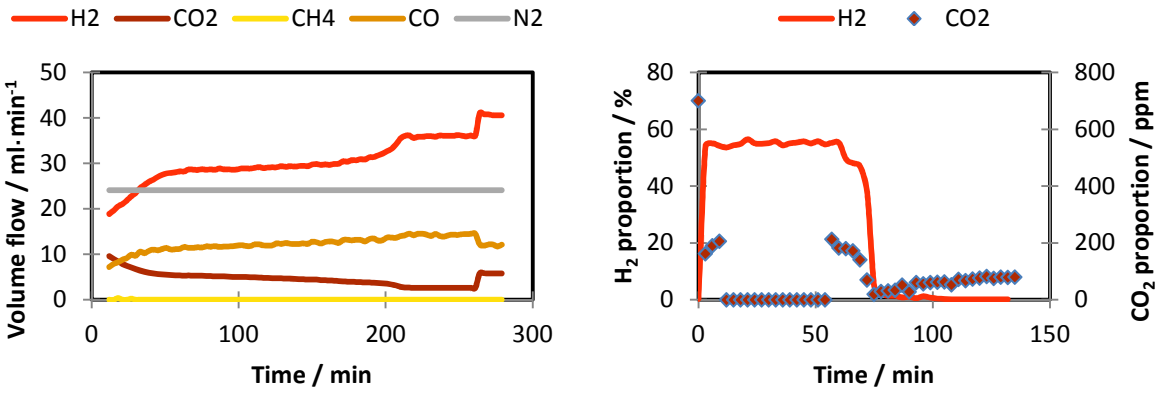


**Figure 55: Reduction with syn-gas mixture (left) and oxidation (right) of the 4th cycle (10th series).**

In this cycle the reduction was performed at 750°C with an artificial syn-gas mixture consisting of hydrogen, carbon monoxide and carbon dioxide. An internal standard of 25 ml/min of nitrogen had to be added for quantification of the reactive gases. Table 20 shows the determined composition of the reducing gas mixture.

A plateau was reached after a period of high conversion. A second plateau after about 215 minutes indicated the occurring side reactions taking over. As discussed in the *ninth experimental series*, this plateau does not correspond to the bypass concentrations. It rather indicates the difference in gas concentrations compared to bypass. The discussed side reactions did occur (Equation 28, Equation 29 and Equation 30). The system was switched to bypass then to compare the gas flows again.

**Table 25: Syn-gas mixture composition (evaluated by bypass).**

| Gas | Flow / ml·min$^{-1}$ | Proportion / % |
|---|---|---|
| $H_2$ | 40.6 | 49.5 |
| CO | 11.6 | 14.1 |
| $CO_2$ | 5.8 | 7.1 |
| $N_2$ | 24.1 | 29.3 |

The oxidation of this cycle was performed with 0.03 g/min of steam in 25 ml/min of nitrogen at pressure greater than 8 bar. As the oxidation could set free the carbonaceous pollutants deposited during the reduction, the GC had to be used for analysis. During this oxidation it was observable that $CO_2$ was emitted to a certain extent also at the beginning of the experiment and also during the end, when there was still a high flow of $H_2$ present.

This possibly allows the assumption that the emission of carbon dioxide is linked to the oxidation state of the contact mass. In this case, the dilution of the $CO_2$ is not the main reason for not detecting any carbonaceous compound during most of the oxidation experiment.

## 3.11.5 Results

Due to the problems of moisture in the first cycle, the results of the second cycle's reduction are not very precise. The third cycle instead showed data quite fitting together. Again, the syn-gas cycle is shown in a separate table (Table 28) and is discussed further downward.

**Table 26: Results of the 10th series.**

| Reaction | $H_2$ / mmol | $H_2$ / ml | $H_2$ conversion / % | $H_2O$ conversion / % | $H_2$ / mmol·$g^{-1}$ | Contact mass conversion / % |
|---|---|---|---|---|---|---|
| Reduction 1 | 86.55 | 1938.66 | 34.05 | - | 14.22 | 84.09 |
| Oxidation 1 | 78.86 | 1768.63 | - | 21.40 | 12.97 | 86.31 |
| Reduction 2 | 60.26 | 1349.92 | 25.28 | - | 9.90 | 65.87 |
| Oxidation 2 | 82.91 | 1857.23 | . | 53.95 | 13.62 | 90.63 |
| Reduction 3 | 70.95 | 1589.19 | 26.81 | - | 11.66 | 77.55 |
| Oxidation 3 | 71.77 | 1607.66 | - | 20.78 | 11.79 | 78.45 |

**Table 27: Reactive gases for syn-gas side reactions, educts marked with *.**

| Gas | Volume / ml | Amount / mmol |
|---|---|---|
| $H_2$* | 457.4 | 20.4 |
| CO | 189.9 | 14.4 |
| $CO_2$* | 321.8 | 0.1 |
| $CH_4$ | 1.9 | 8.5 |

Table 27 offers information on the reactive gases during the proposed side reactions. These values represent the calculated amounts by taking into account the over-productions and over-consumptions by the side reactions. In Table 28 the results of the syn-gas cycle are displayed. High contact mass conversions most certainly have been achieved. These values though are calculated from the calculated values for the amount of reductants $H_2$ and CO. Thus the values are to be seen as a kind of guideline, to visualize the side reactions.

**Table 28: Results of the 4th cycle (10th series), showing the apparent and the side reaction corrected amounts of substance; a [h] indicates the presence of hematite during this reaction. A * during the reduction indicates the total amounts of reductant – $H_2$ and CO are consumed.**

| Reaction | $H_2$ / mmol | $H_2$ / ml | $H_2$ / mmol corr | $H_2$ / ml corr | $H_2$ / mmol·$g^{-1}$ | Contact mass conversion / % |
|---|---|---|---|---|---|---|
| Reduction 4 | 117.48* | 2631.54* | 97.06* | 2174.19* | 16.02* | 94.73[h] |
| Oxidation 4 | 90.47 | 2026.48 | - | | 14.93 | 99.33 |

## 3.12 High Pressure Hydrogen

Investigation of the generation of hydrogen of high purity at raised pressure was one of the main goals of this work. During the initial series operating procedures had changed as well as setup modifications had been done. During the 9th and the 10th series focus was laid on the amount of hydrogen produced during the pressure build-up.

As determined by the setup, there is a direct relation between pressure and amount of hydrogen. Pressure build-up lasted until the operating pressure of 8 bar was reached. This phase is characterized by two periods of different reactivity, indicated by different slopes in the pressure-time diagram (Figure 56). As reactivity declines during the series with the number of cycles, a shift to longer time is visible. The amount of produced hydrogen is always the same as the volume of the system does not change.

For the 9th series this means that the amount of hydrogen produced during the first slope of high conversion decreases whereas the time to reach the operating pressure of 8 bar increases. The two early cycles are comparable as are the two late cycles. A trend of reactivity decrease is obvious.

The 10th series was shorter but is comparable to the previous series. The first and the third cycle are quite similar in the way of pressure build-up not only within the series, but also compared to the early cycles of the 9th series.

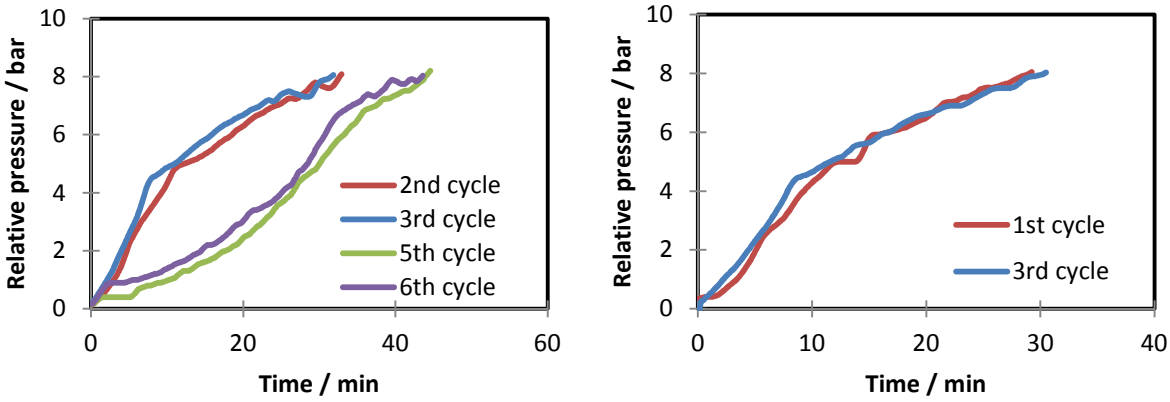


**Figure 56: Change in reactivity in the 9th series over six cycles (left) and in the 10th series over 3 cycles (right) as comparison in pressure build-up.**

The loss of reactivity during the 9th series could either be linked to sintering effects or the formation of channels through the contact mass bed (see *Conclusion*). Both effects would limit the contact area of gas to the contact mass.

# 4 CONCLUSION

Several series of redox cycling of iron oxides were performed during this work. Stabilization and degradation of the contact mass were observable. Pure iron showed the most impressive loss of reactivity. Contact masses with very high amounts of stabilizing agent (20 wt%) showed low volume flows of produced $H_2$. According to this phenomenon, an optimum concentration of $Al_2O_3$ needed to be applied.

The series performed with 5 wt% of additive was able to produce a high amount of hydrogen. The series with 10 wt% performed similar to this. The method of synthesis seems to have no significant impact on the performance of the contact mass. To find the perfect amount of $Al_2O_3$, further experiments are necessary, as during this work just an overview over different amounts could be made.

Additionally to the degradation of the contact mass, the flow pattern of the gases influences the conversion of the contact mass and thus the overall efficiency. The proportion of converted contact mass in most of the cycles is only slightly higher than 55 %. Early series show higher proportions. These relatively low proportions of actually reacting contact masses were related to sintering effects. Throughout the series though, the contact mass conversion did not necessarily decrease. As there were cycles of increased contact mass conversion, the idea of channel formation was born. This means that initially the contact mass bed is packed quite tightly. If now a low gas stream was initiated, gas passed through the bed. If the bed was too tight, larger gas flows would lead to pressure build-up above the bed. The pressurized gas would then force its way through the contact mass by forming channels. These channels would then provide “easier” transgression routes through the bed, leaving wide areas of low gas flows. Further experiments would be needed to compare contact mass conversion to contact mass degradation in more detail.

Direct reduction with methane did not work due to massive formation of solid carbon and thus flow breakdown. The addition of a $CO_2$ fraction could possibly act as oxidant for deposited solid carbon. By use of a gas mixture similar to synthesis gas the reduction can be achieved primarily by the $H_2$ and CO proportion. Because of the occurring side reactions in reduction, the experiments require further experiments. Even the $CO_2$ proportion did not fully prevent the formation of solid carbon, the consecutive oxidation yielded $CO_2$.

The performed experiments indeed proved the value of the steam-iron process. Further experiments should be focused on the cycle stability of the contact mass. The purity of the product gas is paramount, so further experiments should aim for even lower amounts of $CO_2$.

One of the goals of this work was to find and evaluate a method of performing hydrogen generation at raised pressure. The experiments performed provided information on many different aspects not yet described in scientific literature. Pressurization by means of a PID-controlled needle valve proved to be too inflexible. The valve’s controller simply did not react fast enough on changes in gas flow. Thus constant pressure was not possible to maintain. By implementing an additional mass flow controller (MFC) and using it both as a valve for pressure build-up and mass flow meter to detect the product gas flow, constant pressure was easier to achieve. By further improving this setup, the product gas was led into one of the on-board MFCs calibrated for hydrogen. This further increased the comparability of the gas flows. The on-board MFCs were more susceptible to moisture than the previously used system. Further experiments with this setup would need additional effort to separate mois-

ture from the product gas. The on-board liquid-gas separator at about 4°C could not remove enough water from the gas stream – measurement distortion did occur. Even if the MFC is not used for analysis but only as some kind of valve, water still would damage it.

Comparing the cycles of increased pressure with those at ambient pressure gives rise to the assumption that pressurization up to 10 bar has no negative impact on the amount of generated hydrogen. The contact mass reacts to a similar extent comparable to atmospheric conditions.

The analyses of gas mixtures with micro GC was used for the synthesis gas cycles. These experiments provided a more authentic investigation, however a high proportion of nitrogen had to be added as internal standard. This inert gas proportion diluted the product gas stream which possibly prevented the detection of traces of carbonaceous pollutants.

# 5 REFERENCES


[1] International Energy Agency, "Total final consumption," *Key world energy statistics,* p. 28, 2012.

[2] A. Haryanto, S. Fernando, N. Murali and S. Adhikari, "Current status of hydrogen production techniques by steam reforming of ethanol: a review," *Energy & Fuels,* no. 19, pp. 2098-2106, 2005.

[3] S. Subudhi, T. Nayak, N. R. Kumar, P. Vijayananth and B. Lal, "Impact of regulated pH on proto scale hydrogen production from xylose by an alkaline tolerant novel bacterial strain, Enterobacter cloacae DT-1," *International journal of hydrogen energy,* pp. 2728-2737, 2013.

[4] M. C. Williams, "Fuel Cells," in *Fuel Cells: Technologies for Fuel Processing*, Oxford, UK, Elsevier, 2011, pp. 11-26.

[5] T. V. Choudhary and D. Goodman, "CO-free fuel processing for fuel cell applications," *Catalysis Today,* no. 77, pp. 65-78, 2002.

[6] I. P. Jain, "Hydrogen the fuel for 21st century," *International Journal of Hydrogen Energy,* no. 34, pp. 7368-7378, 2009.

[7] J. Ivy, "Summary of electrolytic hydrogen production," National Renewable Energy Laboratory, Colorado, USA, 2004.

[8] K. Onda, T. Kyakuno, K. Hattori and K. Ito, "Prediction of production power for high-pressure hydrogen by high-pressure water electrolysis," *Journal of Power Sources,* pp. 64-70, 2004.

[9] A. Nieto-Márquez, D. Sánchez, A. Miranda-Dahdal, F. Dorado, A. de Lucas-Consuegra and J. L. Valverde, "Autothermal reforming and water-gas shift double bed reactor for H2 production from ethanol," *Chemical engineering and processing: Process Intensification,* no. 74, pp. 14-18, 2013.

[10] J. Adanez, A. Abad, F. Garcia-Labiano, P. Gayan and L. F. de Diego, "Progress in chemical-looping combustion and reforming technologies," *Progress in energy and combustion science,* no. 38, pp. 215-282, 2012.

[11] R. Siriwardane, P. James, K. Chaudhari, A. Zinn, T. Simonyi and C. Robinson, "Chemical-looping combustion of simulated synthesis gas using nickel oxide oxygen carrier supported on betonite," *Energy & Fuels,* no. 21, pp. 1582-1591, 2007.

[12] J. Yoo, Y. Bang, S. J. Han, T. H. Kang, J. Lee and I. K. Song, "Hydrogen production by steam reforming of liquefied natural gas (LNG) over mesoporous alkaline earth metal-promoted nickel-alumina xerogel catalysts," *Journal of Molecular Catalysis A: Chemical,* no. 380, pp. 28-33, 2013.

[13] G. Collodi and F. Wheeler, "Hydrogen production via steam reforming with CO2 capture," *Chemical Engineering Transactions,* pp. 37-42, 2010.

[14] V. Galvita and K. Sundmacher , “Hydrogen production from methane by steam reforming in a periodically operated two-layer catalytic reactor,” *Applied catalysis A: General,* no. 289, pp. 121-127, 2005.

[15] M. Najera, R. Solunke, T. Gardner and G. Veser, “Carbon capture and utilization via chemical looping dry reforming,” *Chemical engineering research and design,* no. 89, pp. 1533-1543, 2011.

[16] F. Mun-Sing, A. Z. Abdullah and S. Bhatia, “Catalytic technology for carbon dioxide reforming of methane to synthesis gas,” *Chemcatchem,* no. 1, pp. 192-208, 2009.

[17] S. T. Oyama, P. Hacarlioglu, Y. Gu and D. Lee, “Dry reforming of methane has no future for hydrogen production: Comparison with steam reforming at high pressure in standard and membrane reactors,” *International Journal of Hydrogen Energy,* no. 37, pp. 10444-10450, 2012.

[18] K. Ghasemzadhe, S. Liguori, P. Morrone, A. Iulianelli, V. Piemonte, A. A. Babaluo and A. Basile, “H2 production by low pressure steam reforming in a dense Pd-Ag membrane reactor in co-currant flow configuration: Experimental and modeling analysis,” *Internatuonal journal of hydrogen energy,* pp. 16685-16697, 2013.

[19] “wallstreet: online,” 6 March 2014. [Online]. Available: https://www.wallstreet-online.de/rohstoffe/palladiumpreis#t:5y||s:lines||a:abs||v:week. [Accessed 6 March 2014].

[20] H. Lane, “The Lane hydrogen producer,” *Flight,* p. 524, August 1909.

[21] A. Messerschmitt.UK Patent 12117, 1912.

[22] M. Thaler and V. Hacker, “Storage and separation of hydrogen with the metal steam process,” *International Journal of Hydrogen Energy,* no. 37, pp. 2800-2806, 2012.

[23] E. Lorente, Q. Cai, J. A. Pena, J. Herguido and N. P. Brandon, “Conceptual design and modelling of the steam-iron process and fuel cell integrated system,” *International Journal of Hydrogen Energy,* no. 34, pp. 5554-5562, 2009.

[24] V. Hacker, “A novel process for stationary hydrogen production: the reformer sponge iron cycle (RESC),” *Journal of Power Sources,* no. 118, pp. 311-314, 2003.

[25] S. Popovic, M. Ristic and S. Music, “Formation of solid solutions in the system Al203-Fe203,” *Materials Letters,* no. 23, pp. 139-142, April 1995.

[26] C. D. Bohn, C. R. Müller, J. P. Cleeton, A. N. Hayhurst, J. F. Davidson, S. A. Scott and J. S. Dennis, “Production of very pure hydrogen with simultaneous capture of carbon dioxide using the redox reactions of iron oxides in packed beds,” *Industrial & Engineering Chemistry Research,* no. 47, pp. 7623-7630, 2008.

[27] H. Topsøe, J. A. Dumesic and M. Boudart, “Alumina as a textural promoter of iron synthetic ammonia catalysts,” *Journal of Catalysts,* no. 28, pp. 477-488, October 1973.

[28] M. Thaler, “Kontaktmassenentwicklung für den Metall-Dampf-Prozess zur Erzeugung und Speicherung von Wasserstoff für Brennstoffzellen,” TU Graz, 2009.

[29] M. Thaler, V. Hacker, M. Anilkumar, J. Albering, J.O. Besenhard, H. Schröttner, M. SChmied, "Investigations of cycle behaviour of the contact mass in the RESC process for hydrogen production," *International Journal of Hydrogen Energy 31,* p. 2025 – 2031, 2006.

[30] C. D. Bohn, "The Production of Pure Hydrogen with Simultaneous Capture of Carbon Dioxide," University of Cambridge, 2010, p. 43.

[31] L. Jin, H. Si, J. Zhang, P. Lin, Z. Hu, Q. Bo and H. Hu, "Preparation of activated carbon supported Fe-Al2O3 catalyst and its application for hydrogen production by catalytic methane decomposition," *International Journal of Hydrogen Energy,* no. 38, pp. 10373-10380, 2013.